Studies on Mathematical Models for Characterizing Plume and Drift Behavior From Cooling Towers

Volume 5: Mathematical Model for Multiple-Source (Multiple-Tower) Cooling Tower Drift Dispersion

EPRI

EPRI CS-1683
Volume 5
Project 906-1
Interim Report
January 1981

Keywords:
Cooling Tower Plumes
Plume Dispersion
Multiple Plumes
Plume Model
Mathematical Model

Prepared by
Argonne National Laboratory
Argonne, Illinois

ELECTRIC POWER RESEARCH INSTITUTE

Studies on Mathematical Models for Characterizing Plume and Drift Behavior From Cooling Towers

Volume 5: Mathematical Model for Multiple-Source (Multiple-Tower) Cooling Tower Drift Dispersion

---

CS-1683, Volume 5
Research Project 906-1

Interim Report, January 1981
Work Completed, August 1980

Prepared by

ARGONNE NATIONAL LABORATORY
Division of Environmental Impact Studies
9700 South Cass Avenue
Argonne, Illinois 60439

Principal Investigators
A. J. Policastro
W. E. Dunn*
M. Breig
K. Haake

*Assistant Professor, Department of Mechanical and Industrial Engineering, University of Illinois at Urbana

Prepared for

Electric Power Research Institute
3412 Hillview Avenue
Palo Alto, California 94304

EPRI Project Manager
J. A. Bartz

Water Quality Control and Heat Rejection Program
Coal Combustion Systems Division

ORDERING INFORMATION

Requests for copies of this report should be directed to Research Reports Center (RRC), Box 50490, Palo Alto, CA 94303, (415) 965-4081. There is no charge for reports requested by EPRI member utilities and affiliates, contributing nonmembers, U.S. utility associations, U.S. government agencies (federal, state, and local), media, and foreign organizations with which EPRI has an information exchange agreement. On request, RRC will send a catalog of EPRI reports.

NOTICE

Prepared by
Argonne National Laboratory
Argonne, Illinois

ABSTRACT

This volume generalizes our multiple-source plume model (developed in Volume 4) to treat drift deposition as well. The basic ideas of drift modeling developed from Volume 3 for single sources are the basis for the treatment of drift in this multiple-tower model. The treatment of droplet breakaway and the treatment of deposition of drift are easily generalized from single-source concepts.

The model is tested with five sets of field data from the Pittsburg, California mechanical-draft cooling towers (MDCTs). The data are the best available for multiple-sources yet these data have several weaknesses. In four of the five data surveys used to test the model, the model predicts sodium deposition rate within a factor of 3 at 50% of all ground samplers. Work continues to determine those conditions under which further simplifying assumptions in the theory may be justified.

EPRI PERSPECTIVE

PROJECT DESCRIPTION

Argonne National Laboratory is performing an effort to develop, improve, and validate mathematical models of cooling tower plumes. Emphasis is being placed on prediction of visible plume trajectory and deposition of saline droplet drift from the tower. Visible plumes and saline drift are environmental impacts of cooling towers that must be considered in power plant siting studies and licensing. A validated mathematical model of plume dispersion provides the industry with the tool required to make an assessment of environmental impact of the cooling tower.

This interim report, in five volumes plus an executive summary, describes results accomplished to date:

Executive Summary--Overview
Volume 1--Review of European Research
Volume 2--Single-Source Model
Volume 3--Drift Modeling of Single Sources
Volume 4--Multiple-Source Model
Volume 5--Drift Modeling of Multiple Sources

In a continuing effort, emphasis is being placed on developing a master model that is user-oriented and designed specifically for siting and licensing studies.

PROJECT OBJECTIVES

The goal of this effort is to develop, improve, and validate mathematical models of cooling tower plume dispersion for individual and clustered mechanical- and natural-draft cooling towers. The overall goal is to provide the utility planner with a tool for studies involving the environmental impact of cooling tower plumes.

PROJECT RESULTS

A model that has been developed and validated has prediction capabilities that are superior to other available mathematical models of cooling tower plume dispersion.

For example, in 77 percent of all cases of single sources that were studied, the model predicted a visible plume rise within a specified accuracy. This was the best performance among all available models (over a dozen) that were investigated.

This effort has also produced a useful review and summary of European research on cooling tower plume dispersion (Volume 1). Workshops in the fall of 1981 and in 1982 are being planned to disseminate to the industry the computer code that is being developed.

This series of volumes should be of value to utility planning engineers concerned with the impact of cooling tower plumes on plant siting.

John A. Bartz, Project Manager
Coal Combustion Systems Division

ACKNOWLEDGMENTS

The authors of this report would like to extend their appreciation to Dr. Nels Laulainen of Battelle Northwest Labs and Dr. Ron Webb of Environmental Systems Corporation for their cooperation in responding to our numerous questions concerni the Pittsburg, California field data. We would also like to thank Dr. John Bartz of EPRI for his continued support and encouragement as technical monitor for the project. Finally, we would like to thank Dr. George McVehil for the many helpful comments and suggestions he made on a draft of this volume.

ILLUSTRATIONS

TABLES

SUMMARY

This volume generalizes models developed in Volume 3 (single source drift model) and Volume 4 (multiple source plume model). The result is a model that can treat both plume rise and drift deposition from multiple sources. The model applies to multiple NDCTs or multiple MDCTs and can handle wind direction at any angle with the line of towers.

Existing models for drift deposition from multiple sources all employ the equivalent source concept in which all cells or towers are combined into a single source of equal mass, momentum, and energy flux. This simplification is convenient but is not proven to provide correct predictions. We expect that the equivalent source concept will have its greatest errors in the near and intermediate field when individual plumes are still present and important since merging is not complete. The equivalent source concept may be adequate in the far field yet this is not assured.

The model presented here uses our multiple source plume code presented in Volume 4. The drop evaporation formulation developed in Volume 3 is also used unchanged. A special simplification is added in which our droplet evaporation subroutine need only be applied to droplets from the first source; droplet evaporation results are saved and used to approximate evaporation of drops from the other sources, depending on breakaway height. Droplet breakaway is generalized (using the radius criterion, see Volume 3) to merging plumes by simply using the merged plume characteristics (after merging has occurred) in the tracking of drops from each source. Droplet deposition is generalized from the sector-averaged approach by employing a Gaussian distribution (function of angle θ) to spread droplets (for any given bin) laterally from the wind direction after deposition. The complete model includes several simplifications and devices in order to provide economical computer run times.

The field data at Pittsburg, California are used to test the model. Data on ground-level sodium deposition flux are compared to model predictions.

The plant has two towers of 13 cells each. Although these data are the best available, they have several inadequacies

(a) only a single droplet spectrum and tower liquid emission rate are provided to represent source conditions for all days experiments were made

(b) significant discrepancies exist in the measured data for the total salt emitted from the tower. Measurements were made by the isokinetic sampler and compared to the value obtained from integrating over the drop spectrum assuming each drop has the basin salt water concentration

(c) ambient profiles of wind speed, humidity, and temperature are periodically taken for some dates; on other dates, measurements at ground-level only are provided.

(d) large variations in wind direction with height and with time make a single choice of wind direction per hour difficult. This is a model problem rather than a data problem.

(e) wind speeds were quite large and led to smearing of drops on sensitive papers at ground level. This raised questions as to the accuracy of drop size measurements made.

Model/data comparisons revealed that except for one case (of five), our model predicted sodium deposition within a factor of 3, for 50% of all samplers over the four survey dates. Future work will involve an attempt to determine under which multiple-tower conditions, simplifications in the model (and computer code) are warranted.

Section 1

INTRODUCTION

This volume combines the models developed in Volumes 3 and 4 into a generalized model capable of predicting both plumes and drift from multiple-tower configurations. These configurations could be sets of natural- or mechanical-draft cooling towers. Volume 3 presented a model for drift deposition from single sources encompassing plume rise, droplet breakaway, droplet evaporation, and droplet deposition submodels. Volume 4 expanded the plume rise model to handle multiple sources. In this volume, the multiple-source plume rise model is used as a base for which generalized breakaway and generalized deposition formulations are combined with our droplet evaporation formulation to provide a generalized plume/drift model.

As we will see, this generalization to a multiple-source plume/drift model is quite natural based upon previous models and submodels developed. Here we need only provide details on our methodology for developing the generalized breakaway and generalized deposition treatments in order to fully define our multiple-source drift model. Section 2 provides the required model development information.

Section 3 provides validation of the model with field data from the Pittsburg, California mechanical-draft cooling towers. The data are the best available, yet have a number of important limitations. In any case, our model performs fairly well with those data as will be seen in Section 3.

It should be recognized that existing models for multiple-source drift deposition provide an overly-simplified treatment of NDCT or MDCT drift deposition predictions. No model that we are aware of treats the effects of drift dispersion from individual cells or towers. In general, existing models employ a combined source approach whereby all cells and towers are combined into one large source from which the entire plume and drift emission occurs. This generally is a very poor assumption in regions in the near and intermediate field of the tower. It is done for simplicity with no proof to support it. Such an assumption combining all cells into an equivalent source will necessarily lead to a single large plume which will rise higher than the plumes from the individual cells and, as a result,

will have notably different plume characteristics. It is highly unlikely that drift characteristics will be unaffected by that simplifying assumption. We expect that the equivalent source concept will lead to higher-rising plumes, higher droplet breakaway locations with deposition occurring further from the tower.

We recognize the need to provide some treatment for individual plumes and the effect of wind direction on plume rise and drift deposition. However, we also are well aware that our resulting model must remain economical to run. As a result, we have employed a few devices to significantly reduce computer time for our code and still have the code provide the advantages of treatment of individual plumes and the handling of the effects of wind direction on plume/drift dispersion.

Section 2

DEVELOPMENT OF THE ANL MULTIPLE-SOURCE DRIFT DEPOSITION MODEL

INTRODUCTION

The ANL multiple-tower drift model was developed as a straight-forward generalization of the ANL multiple-tower plume model employing concepts used in the ANL single-tower drift model. Only two areas require generalization to multiple-source applications: (a) the methodology of the treatment of droplet breakaway after plume merging, and (b) the methodology of drop deposition generalizing the sector averaging concept; that concept is applicable only to single sources.

Items taken directly from previous work are

(i) the multiple-source plume model (from Volume 4). This plume model is needed to transport drops from each cell (MDCT) or tower (NDCT) downwind until they break away from the plume,

(ii) the droplet evaporation submodel (from Volume 3) which is applicable to all drops from all towers and is applied after drop breakaway. Items (a) and (b) will be discussed below. In addition, a final item involving methodology for reduction of computer time will be discussed.

GENERAL OPERATION OF THE COMPUTER CODE

In this section, the process of computation of drift deposition is described. Discussion items listed above will be provided subsequently.

For a particular observation which includes ambient profiles and tower exit conditions (plume and drift), the plume model is set into operation. For each step in plume calculations, the emitted drift droplets from that cell or tower are followed along with the plume. Thus for each plume step, we employ at least one step in our drift drop integration to allow droplets to keep up with the plume. .In actuality, the code stores only plume information from three consecutive plume steps at a time. Information for older plume steps are printed in the out-

put but are not stored. All droplets are followed within the plume until they are within the plume region bounded by those three planes or else have broken away.

The reason for storing plume information at three planes and not just one plane is as follows. We recognize first that droplets being followed from one cell or tower will not all be at the same x (downwind location) or z (vertical location) after a given number of droplet integration steps. Clearly, droplets have different settling velocities whereby the heavier drops will have a lower rise and be subject to generally smaller wind speeds as they disperse. An additional complicating feature is that plume variables are computed by the plume model at planes normal to the centerline and not normal to the wind. These two factors cause some droplets to fall behind others in their x and z locations after equal numbers of integration steps for the drift droplets. The larger drops will tend to lag behind and lie in earlier plume planes of integration. We therefore take extra steps of integration for the larger drops in order to have them keep pace with the smaller drops. We find that storing three planes of plume results and following the larger drops with occasional additional steps until they were within those three planes was a cost-effective measure.

In addition, it is inefficient to compute the entire plume and its characteristics, save all results at all cross-sections, and then go back to the tower outlet and compute the trajectory of each drift droplet through the already-computed plume. We achieve considerable storage savings by computing drift trajectories as we are computing the plume, allowing drops to fall out as we compute.

Recall that the multiple-source plume model is set up to first compute the plume from the most upwind source. The model then follows that plume until we are at the downwind location of the second most upwind source, computing that plume, etc. allowing for plume mergers as we compute. This procedure is unchanged in the multiple-source drift application except that now we compute drift characteristics of each source we are following at the time we compute the plume spreading.

TREATMENT OF DROPLET BREAKAWAY

The methodology employed here is a generalization of the single-source method whereby drops are assumed to break away from the plume as soon as they have fallen below the plume radius. To apply this thinking to multiple source plumes, several flags are maintained in the computer code to assist decision making. These flags describe the condition of the plume from each cell or tower, and determines such

features as (a) whether the plume has appeared (begun to be calculated), or merged and became part of the major plume, or merged with one of the minor plumes, and (b) which major plume that cell's plume has merged with, if any.

The basic method of following droplets during merging is the following: when one plume merges with another, drop trajectories from either plume are followed using the merged plume characteristics (radius, U, V, W). At the beginning of the diffusion phase for any plume, all remaining drops (that have yet to break away) are assumed to break away.

METHODOLOGY FOR TREATMENT OF DROPLET DEPOSITION

After all drops from all towers have been deposited on the ground, we call a subroutine SECDEP to compute the salt deposited (in kg NaCl/m^2-hr), the number drop deposition (in # drops/m^2-hr), the salt concentration in the air (in kg/m^3), and the drop solution deposited (in kg solution/m^2-hr). For single tower cases, we set up a 22 1/2° or 15° sector about the wind direction and distribute the deposition (salt, water, no. of drops, etc) evenly within annuli bounded by the sector and radii determined by the locations where consecutive drops in the drop spectrum strike the ground. However, this concept does not generalize directly to situations with multiple cells or towers because there is no common origin for all sources. The idea of the 22 1/2° or 15° sector has no real meaning.

The sector concept can be generalized easily if one reflects on the real meaning of the sector concept. We begin by setting up a Gaussian curve centered about the wind direction. The Gaussian is a function of directional angle from the cell that the drops were originally emitted (see Fig. 2-1). For example, let R_1 and R_2 be the deposition distance of two consecutive drops in the drop spectrum from a particular cell (MDCT) or tower (NDCT) where sampler k is located between R_1 and R_2. For each observation period of calculation, the fraction of salt drift deposited is computed for sampler k from

$$\text{SALNEW} = \text{MASFRAC}\ (I) \cdot \text{DRIFTR} \cdot \text{CWSC} \cdot \text{ONN}(k) \cdot (A/B)$$

where

$$A = e^{-(\theta^2/2\sigma_x^2)}$$

$$B = \sigma_x\ (R_2^2 - R_1^2) \cdot 1.253 \times 10^3$$

MASFRAC (I) = the mass fraction in the drop spectrum for the droplet range (I, I + 1)

DRIFTR = drift rate from cell (MDCT) or tower (NDCT)

CWSC = cooling water salt concentration

ONN(k) = amount of time sampler k is on during this particular observation

σ_x = sector size (22 1/2°) in radians

θ = angle measured clockwise or counter-clockwise from the wind direction in radians

1.253×10^3 = units conversion factor

From this equation, the salt to be deposited between radii R_1 and R_2 get distributed in a Gaussian manner about the wind direction. After salt deposition from each meteorological observation is calculated, the summed value of all the SALNEW's is divided by the summation of time each sampler was on in order to get a final weighted value for salt deposited.

It is worthwhile here to review again (see Volume 3) how calculations are made when the total time of calculation is divided into specific (short) periods as we are intending here. As each meteorological observational period (30 minutes, one hour, for example) is processed by the model, the amount of time each sampler is operational (on) for that observation determines the sampler on-time. That sampler on-time pro-rates the contribution that each observational period provides to the total period of data measurement.

COMPUTER TIME-SAVING FEATURES

There are several methods we use to significantly reduce computer-run time of our model. Most have no effect on final predictions. The last one described here (in (c)) we believe has insignificant effects on final calculations based on limited testing carried out to date. The short cuts are based on the following

a) any drop emitted from the tower which is smaller than 80 μm in diameter is not generally followed in the code unless specifically requested on input. Droplets that small will surely deposit at distances farther from the tower (>10 km) than we are generally interested in computing

b) once a drop emitted from the tower deposits beyond the furthest sampler (known from input), we know that all smaller drops from that plume will deposit

even further and have no impact on any of our ground samplers. As a result, we discontinue following all smaller drops no matter at which airborne locations they may be.

c) our droplet evaporation subroutines are only applied for the first cell (MDCT) or tower (NDCT). (Our model assumes identical drift spectra at tower exit for all sources). All deposition distances from all other cells and sources are calculated from the deposition information obtained from source #1 along with the breakaway coordinates for the other source. This is an approximation, of course, which appears to be a fairly good one for the cases we tested.

A description of this approximation is given below.

During each observation, every drop from every cell (except drops under 80 microns and large drops that are too large to escape from the tower) has its trajectory calculated to the point of breakaway. As noted above, only drops from cell #1 are sent through the DROP subroutine for calculation of final deposition distance. Since final diameter and settling velocity for a drop was approximately the same for each cell (tower), the final deposition distance is determined for each cell (other than #1) from deposition distance for that same drop for cell #1 and the breakaway coordinates XREL2, ZREL2, for both cells. The approximate equations, used for the final deposition distance of a certain drop for cell J, become from linear interpolation:

$$\frac{ZREL2(1) + HGT}{Depox\ (1) - XREL2(1)} = \frac{ZREL2(J) + HGT}{Depox\ (J) - XREL2(J)}$$

$$Depox\ (J) = XREL2\ (J) + \frac{ZREL2(J) + HGT}{ZREL2(1) + HGT}\ (Depox\ (1) - XREL2(1))$$

where

HGT = tower height,
XREL2(J) = distance to breakaway of a fixed drop for cell J,
ZREL2(J) = height of breakaway for a fixed drop for cell J, measured above the tower top.
Depox (J) = downwind distance (in x direction) to deposition for cell J

Index 1 refers to the same quantities for our drop of interest for cell #1.

These equations represent linear interpolation (or extrapolations) based upon released heights and deposition distances known for the same size drop at the first cell and the cell of interest.

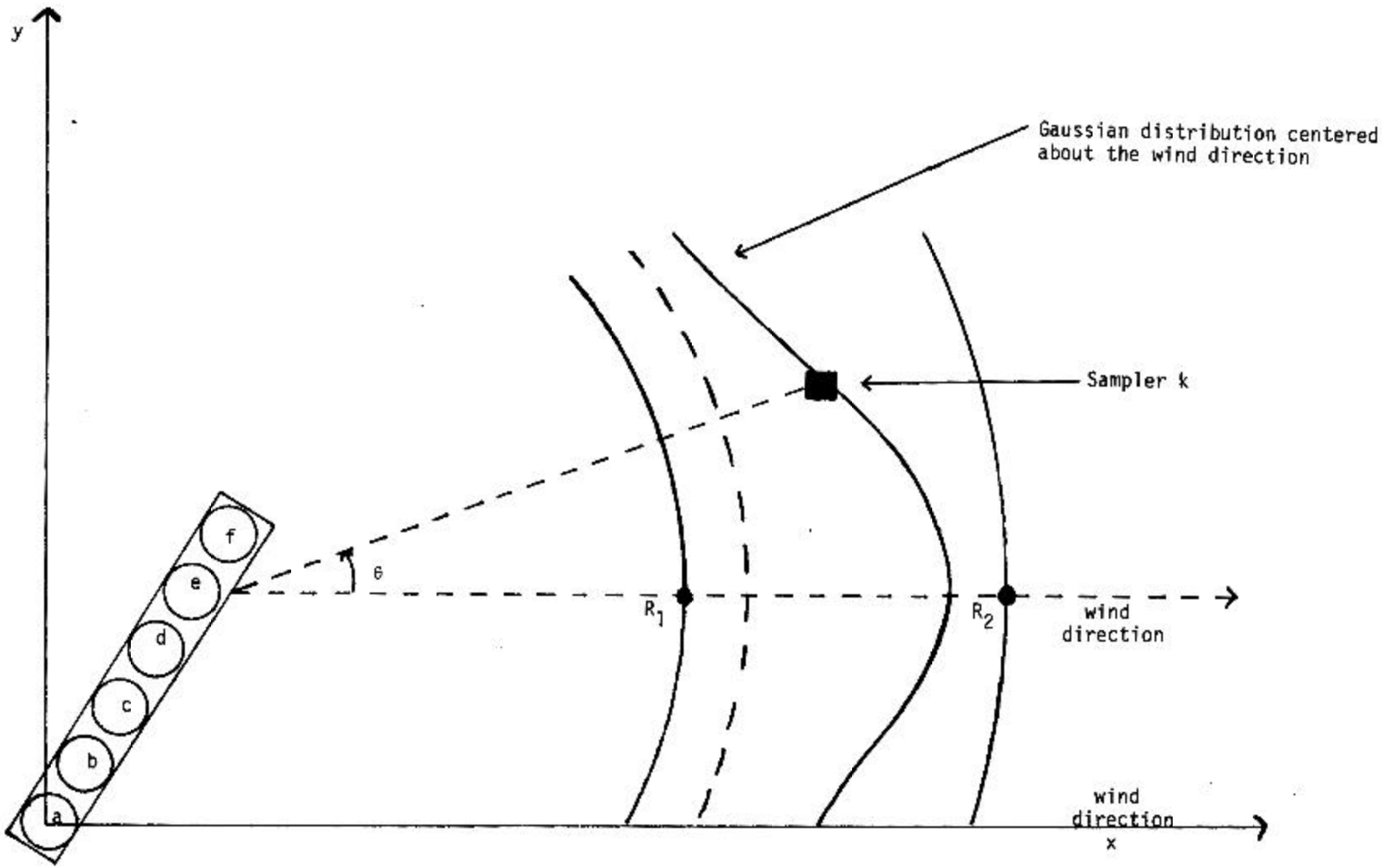

Figure 2-1. Example of Gaussian distribution scheme used to disperse droplets laterally upon deposition. Sampler k is between droplet deposition distance R_1 and R_2 for two consecutive drops in the drop spectrum from cell e.

Section 3

MODEL VALIDATION WITH PITTSBURG, CALIFORNIA FIELD DATA

INTRODUCTION

The only complete sets of field data on multiple source drift deposition exist from the field study (1) done at the Pittsburg, California MDCTs. These data will be described in some detail in the next section. The data provide a test of our model for multiple-source drift emissions. As will be seen, the data contain several weaknesses, many of which represent inherent difficulties in collecting the needed input to a model from a complex system of sources. As a result, significant uncertainty surrounds the input data, and to some extent the deposition data as well. These uncertainties becloud the model/data comparisons somewhat. In any event, model performance is quite reasonable as will be seen; this fact provides not only some verification for the model but also to the data as well.

It should be emphasized that several field surveys from a single site do not provide final verification for any model. Indeed, measurements at Pittsburg, California were generally taken under high wind conditions and do not represent a wide range of ambient conditions for that site. Moreover, the data were acquired only within 1 km of the towers and no further. As a result, models will not be able to be verified at distances greater than this with these data. Since no other multiple-source data exist for any site, the model remains unverified at those larger distances. The correctness of the model for those distances must be based upon theoretical validity of the model.

DATA MEASURED AT PITTSBURG, CALIFORNIA

The entire field study is described in detail in (1). The source measurements are described in detail in (2). A brief description of the pertinent data for model application is given here.

The plant consists of seven oil-fired units. Units 1-6 employ once-through cooling, while Unit 7 (rated at 720 MWe net) is cooled by two 13-cell

Marley rectangular mechanical draft cooling towers located, approximately 0.5 km from the unit, on the center berm in a cooling canal west of the plant. Figure 3-1 provides a sketch of the site. The two cooling tower units are identified as Tower 7-1 and Tower 7-2; Tower 7-2 is about 325 m west of Tower 7-1 measured from center to center. Individual cells are numbered 1-13 from west to east. Cell exit diameter is 10 m with the exit plane 5.5 m above the fan deck and 18 m above ground level. The canal was previously used as a spray canal for Unit 7. The towers were stated to have a guaranteed drift rate of 0.004% and a normal circulating water flow of 23.5 m^3/s. One problem is that there are leaks around the cooling tower drift eliminators which, for certain cells, allow for significantly higher drift emissions than for other cells. Total dissolved solids concentration of the canal water was found to vary over several orders of magnitude over the year, with sodium ion concentrations varying between 0.01 and 1.5% by weight.

Eight field surveys of drift were conducted during the June 1978 drift study at Pittsburg, by Battelle Pacific Northwest Laboratories with assistance on source measurements by the Environmental Systems Corporation.

Downwind deposition measurements were coordinated with ESC's source measurements on the first seven tests. The eighth test was conducted with no concurrent source measurements. The tests were divided into two-tower operation (three tests), Tower 7-2 alone (two tests), and Tower 7-1 alone (three tests).

Meteorological conditions indicated significant winds on most days that tests were made. The winds, though persistently from SW to W to NW, were more intense during the morning hours than usual. Only two test runs were made where the wind speed could be classified as 5 m s^{-1} or less. The other tests were carried out under conditions where wind speed ranged from 5 to 10 m s^{-1}. A summary of the test runs and average meteorological conditions is found in Table 3-1.

For characterization of cooling tower source emissions, measurements of droplet size, mineral mass flux, updraft air velocity and updraft air temperatures were performed by ESC using the following instrumentation:

- Sensitive Paper System (SP),
- Particulate Instrumentation by Laser Light Scattering System (PILLS II),
- heated Glass Bead Isokinetic Sampling System (IK),
- Gill propeller anemometer,
- electronic psychrometer.

Samples of the circulating water were also acquired from the hot water basin of the cell under measurement for later chemical analysis of the mineral tracers, which include sodium and magnesium. In this way the droplet salt concentration emitted by the towers could be determined, assuming of course that the emitted droplets have the same salt concentration as does the basin water.

Clearly, it is infeasible to measure drift spectra and cell exit conditions from all cells on every day of the tests. As a result, a series of pre-test measurement were conducted on all operating cells over a 2-day period (June 13-14, 1978) before the intensive tests were begun in order to rank the emissions on a cell-to-cell basis. In this way, a reduced number of cells would have to be measured daily. The basic assumption made, which proved true, was that cell-to-cell differences in drift emissions were far greater than same-cell differences on a day-to-day basis. Thus, measurements of one typical cell's drift changes over a day-to-day basis should, hopefully, characterize the entire towers' changes in daily drift emissions.

First, the relative ranking of the respective cells will now be presented (Figure 3-2). On June 13-14, 1978, each of the 26 cells (except fans 5, 10, 13 on tower 2 which were not operating), had the following measurements made:

(a) visual examination of drift eliminator condition and droplet discharge through leaks,

(b) visual examination of drift at the fan stack exit plane,

(c) droplet Sensitive Paper exposures for relative ranking of cell emissions.

Visual examination of the exposed Sensitive Papers was used in ranking the cells in these categories: High, Medium, and Low drift emissions. The following rankings resulted from examination of the SP's.

		High	Medium	Low
Tower 7-1:	cell #	3	1, 2, 4, 5-7, 10-13	8, 9
Tower 7-2:	cell #	4, 9, 11, 12	1-3, 6-8	-

Table 3-2 lists the dates of the comprehensive tests noting the specific cell on the dates indicated which was measured completely. Note also, that on most dates, reference cells 1-7 and/or 2-7 were spot checked. Spot checks were made with 142 mm Sensitive Papers but at only 4 positions across the cell. For a comprehensive measurement, 12 locations were generally used. Limitations arising from those measurements are noted in the next section. Results from the reference cells did show that drift mass flux can vary day-to-day by as much as an order of magnitude for the same measurement position.

At present, it is not known whether the day-to-day differences noted from the reference cells were due to real changes on a daily basis or due to the limited number of sample points and sample duration of the SP's. ESC recommends (3) that due to sparse sampling, that modelers employ a single-composite drift droplet spectrum for calculations independent of date. ESC set up this single spectrum using a weighted average of those cells judged during the pretest survey to have high, medium, or low emissions. The representative spectrum is listed in Table 3-3 and presented in Figure 3-3. The mass peak near 30 μm probably represents droplets from the fill that have passed through the drift eliminators while the mass peaks at 300 μm and beyond are probably the result of large droplets formed by leakage of water into the tower plenum.

The emission rate per cell was found to be 4.8 g s^{-1} resulting in a total emission rate of 124 g s^{-1} if all 26 cells are operating. This weighted value is also recommended (3) to be used by modelers as a fixed value, independent of day of survey. The total emission rate corresponds to a drift fraction of 0.0006% for a total circulating water flow rate of 20 m^3 s^{-1}. The measured drift rate is consistent with results of other measurement programs on modern cooling towers that have current drift eliminator design.

Meteorological conditions were quite similar during the test period. Generally fair weather prevailed with clear skies, warm temperatures, and moderate-to-high winds. Since all the test runs except for test run 3, dated June 15, 1978, were conducted during the morning hours, surface temperatures increased from an average low value of about 15°C at the beginning of a test

run to an average high of about 23°C at the end of it. Relative humidities decreased from ∿75% to ∿50% during the same time period. Winds generally increase by 1-3 m s^{-1} with an average value during the test period of about 6 m s^{-1}. Wind direction was from the west (270°) during the first three test days, but was from the WSW (∿245°) for the remainder of the test period. Standard deviations of wind direction were quite low, typically $\lesssim$10°.

A 10-m met tower recorded dry-bulb temperature, relative humidity, and wind speed/direction. Ten minute and hourly averages were presented.

Vertical profiles of temperature, wind and relative humidity were also derived from the tethered balloon system measurements. Generally, wind speeds were too great to effectively use that system. In any case, we used the vertical profiles for model input when available and the 10-m met station results otherwise. See Table 3-4 for ambient information that we used in our model.

Mineral concentration of the cooling tower circulating water increased dramatically during the field test. Sodium ion concentration derived from chemical analysis of circulating water samples collected by ESC and PNL are shown in Figure 3-4 and Table 3-5. Values calculated from PG&E's cooling tower water analysis, assuming that Na^+ represents 34% of the salts in seawater, are also shown. Mineral ion ratios, referenced to Na^+, are listed in Table 3-5 for completeness. Conversations (4) with Laulainen of PNL resulted in a recommendation that we use the average of ESC and PNL measured values for cooling water salt concentration for a given survey period.

An explanation to account for all the observed changes in sodium concentration during a given test run and changes in the mineral ratios is lacking at the present time. Either makeup and/or blowdown rates were not as stated or the canal water was not uniformly mixed or the makeup water from Suisun Bay exhibits large diurnal variations in mineral ion concentration. The latter explanation is probably correct because of tidal action. Incoming tides would bring in salin water from San Francisco Bay while outgoing tides would result in dilution by fresh river water.

Table 3-6 lists the locations of ground samplers for the study. Sensitive papers were used to record droplet sizes and numbers whereas bulk deposition samples were used to provide data on mineral ion deposition rates.

LIMITATIONS OF THE FIELD DATA

The following are limitations in the data which we should be aware of in evaluating our model/data comparisons. Some of these limitations relate to the difficulties inherent in providing measurements for multiple cooling towers. Other limitations relate to the special (and difficult) meteorological conditions on the dates of the experiments. The third set of limitations relate simply to uncertainties in the numerical values of the data and to data oddities.

Limitations relating to model input are:

(a) a single drop size spectrum and tower liquid mass emission are recommended by PNL and ESC and are assumed to be unchanged for all dates of the field study. Clearly, this is unlikely to be the true situation but such an assumption was the best one that could be drawn from the source data measured. With 26 cells and the ability to measure only one cell per date in detail, it was not possible to provide an accurate spectrum and drift emission rate on a day-to-day basis. The attempt to evaluate drift emission changes on the towers by looking at the reference cells on a day-to-day basis [by using 4 SP's] was not successful due to the small number of SP's used.

(b) the amount of salt emitted by the tower is not known precisely due to the classic controversy over the accuracy of the isokinetic sampler. Table 3-2 presents the ratio of IK measured salt emission rates versus salt emission rates computed from the drop spectrum assuming that each drop contains the same salt concentration as the basin water. ESC believes that the difference is due to evaporation within the tower. In any case, the uncertainty remains significant.

(c) the basin water salt concentration also remains uncertain due to the fact that different measurement methods (see Table 3-5) yielded widely differing values on many of the days. N. Laulainen of PNL recommended that we average the PNL and ESC measured concentrations.

(d) uncertainties exist in the size of the droplets striking the SP's located at the ground due to the large wind speeds that were present on most survey dates. Many drops created an irregular water mark on the SP (Figure 3-5) which made it difficult to assess the drop diameter just before deposition. ESC

developed a new calibration procedure in an attempt to estimate the drop diameters before deposition. Our model/data comparisons used, instead, bulk deposition rates of sodium as tests of model performance.

(e) In most cases, ambient profiles of wind, humidity, and temperature, were measured vertically. In other cases, however, only ground-level measurements were made. In total, the Pittsburg, California drift data include five cases where all necessary model input data were measured and where ground-level drift data were consistent to a reasonable degree. These dates were:

(1) June 16, 1978 / data denoted PITT 16
(2) June 17, 1978 / data denoted PITT 17
(3) June 18, 1978 / data denoted PITT 18
(4) June 21, 1978 / data denoted PITT 21
(5) June 22, 1978 / data denoted PITT 22

Cases PITT 16, 17 and 21 have a more refined ambient meteorology than the other two cases due to the fact that ambient profiles were measured on those dates. A single reading at 10-m above the ground is the sole ambient information provided the other two dates. The assumption of constant wind with height is a poor assumption near the ground. As a result, we assumed a 1/7-power law to extrapolate 10-m level winds and, in addition, assumed a neutral lapse rate for temperature.

(f) Drift deposition data reveal some inconsistencies which raise questions concerning some of their validity. We will take each data case separately for discussion. Refer to Figures 3-6 to 3-10 and Tables 3-7 to 3-11 for better understanding of the following discussion. Also note each case run is broken into several observations to allow for changing meteorological conditions during a case.

PITT 16 This case has four arcs with samplers turned on. In arc 0, the wind is directed towards samplers OBN and OBS for two observations, and then the wind is directed towards OC and OD for two other observation periods. The observed values of sodium deposition for this arc appear inconsistent since (a) OBS has a much smaller amount of sodium deposition (31 $\mu g/(m^2\text{-hr})$) than OBN (112 $\mu g/(m^2\text{-hr})$) and (b) sampler OD appears to have an extremely large amount of sodium deposition (192 $\mu g/(m^2\text{-hr})$) compared to sampler OE next to it, which gets zero deposition.

Also, in arc 1, sampler 1E must have given inaccurate measurements since it gets zero deposition while samplers on both sides record fairly large amounts of sodium deposited. Also, in arc 2, sampler 2G appears to have given an erroneous value of zero deposition whereas the sampler next to it (2H) seems to have too high a deposition rate (between 5 and 36 $\mu g/(m^2\text{-hr})$) relative to the other samplers in this arc. Arc 3 has several samplers: 3A, 3B, 3C and especially 3E with larger amounts of deposition relative to their distance from the source (compared to deposition at samplers closer to the towers). It appears unreasonable for sampler 3E to receive a very large amount of deposition whereas sampler 3F, which is very close, gets zero deposition.

PITT 17 This case has only one tower in operation and four arcs with samplers operational. In arc 1, samplers 1C and 1F are both in the direction of the wind yet they receive zero deposition, whereas samplers 1D and 1E collect a considerable amount of sodium. Also, in arc 1A, sampler 1AC like sampler 1C collects very little sodium while other samplers farther off from the centerline trajectory of the plume (and wind direction) receive more sodium. In arc 2, sampler 2F has one reading (17 $\mu g/(m^2\text{-hr})$) which is a little high. In arc 3, both samplers have high amounts of deposition measured relative to distance from the tower, as compared with deposition values measured closer to the source.

PITT 18 This case has one tower operating and three arcs with samplers on. Arc 1 has one sampler (1C) which appears to collect more sodium than it should relative to other samplers in this arc that are more in line with the wind. In arc 1A, sampler 1AC (like 1C) collects more sodium than some of the other samplers in this arc. For example sampler 1AZ, which is in the line of the wind for most of the time this case is running, collects 5 $\mu g/(m^2\text{-hr})$ while 1AC which is never directly in the line of the wind collects 71 $\mu g/(m^2\text{-hr})$ of sodium. In arc 2, samplers 2A and 2B should receive fairly even amounts of sodium yet 2A collects much less sodium than 2B.

PITT 21 This case has one tower in operation and four arcs with samplers. Arc 0 has one questionable data point, OBN, which collects more sodium than OA does whereas OA is more in the direction of the wind for the entire duration of this case. Arc 1 reveals several inconsistencies in the data. Sampler 1ZZ collects a large amount of sodium (240 $\mu g/(m^2\text{-hr})$) whereas sampler 1Z, located directly behind sampler 1ZZ (100 m distant), collects zero deposition. Samplers 1B and 1C behave much like OBN as they collect more sodium than they should as compared

to deposition at samplers 1Z and 1A. Arc 1A has two samplers again (1AB, 1AC) that collect more sodium while being farther from the direct line of the wind. Finally, Arc 2 reveals two samplers with inconsistent data. The samplers are fairly close yet sampler 2A gets zero deposition whereas 2B gets 89 $\mu g/(m^2\text{-hr})$), a very large amount of sodium relative to distance from the source.

PITT 22 This case has four arcs and has both towers operating. Arc 1 has one questionable point; sampler 1Z collects zero deposition whereas the sampler right in front of it (sampler 1ZZ) collects a large amount of sodium, 78 $\mu g/(m^2\text{-hr})$, (just as in case PITT 21). Also, as in case PITT 21, arc 2 has 2 samplers again with inconsistent results. Sampler 2A collects zero deposition whereas sampler 2B collects between 102 and 20 $\mu g/(m^2\text{-hr})$ again a very large amount of deposition relative to distance and deposition of closer-in samplers.

RESULTS OF MODEL/DATA COMPARISONS

Tables 3-7 to 3-11 summarize the model/data comparisons for our five dates. Figures 3-11 to 3-20 plot the predictions versus the data for each arc on each date. Table 3-12 summarizes the model/data comparisons in terms of several simple statistics. Note that except for PITT 16, where model/data comparisons appear to be completely anomalous, the model predicts deposition within a factor of 3, 50% of the time. We believe this is quite good considering the simplications made in the model and the questionable areas relating to the data themselves. Please note that the model predictions generally are low outside the main wind directions, build up to a peak somewhere near the main wind direction and then taper off as the wind angle deviates more and more from the main wind direction. This Gaussian type shape is due to fluctuations in the wind direction about the main direction during the data survey. The data do represent that shape although in a rough manner at times.

In some cases, the peak deposition appears to have been captured in the data. For instance, for the June 22, 1978 data, the peak appears in all three arcs and is predicted by the model but the predicted peak is about 0-30° off depending upon arc chosen. Our model accepts only one wind direction to be used for all heights. That value was chosen as the value at tower top. Clearly, the data show (when profiles are measured) that the wind angle can vary greatly with height and that a single value may not be very representative. This variable is

indeed a difficult parameter to pin down to a single value with height. Inaccuracies in the choice of this angle does have some effect on model predictions. We evaluated (not shown) the effect of different choices of wind direction per meteorological observation period. We noted, for instance, that use of an average of the wind directions over the height of the plume (instead of using the tower top value) would not provide significantly better predictions or help explain the data discrepancies described earlier.

REFERENCES

1. N. S. Laulainen, R. O. Webb, K. R. Wilber, S. L. Vlanski. Comprehensive Study of Drift From Mechanical Draft Cooling Towers. Battelle Pacific Northwest Laboratory. EY-76-C-06-1830. Richland, Washington. September 1979.

2. R. O. Webb. Drift Measurements from Mechanical Draft Cooling Towers. Cooling Systems Project Group. Environmental Systems Corporation. Knoxville, Tennessee. October 1978.

3. R. O. Webb. Personal Communication. Environmental Systems Corporation, Knoxville, Tennessee. July 1980.

4. N. S. Laulainen. Personal Communication. Battelle Pacific Northwest Laboratory. Richland, Washington. July 1980.

Table 3-1

Summary of test runs and average meteorological conditions during the June 1978 Pittsburg Drift Study

Date	Run No.	Temperature (°C)	Relative Humidity (%)	Wind Speed (ms^{-1})	Wind Direction (°)	Comment
6-15	3	23.6	43	6.6	292	Both towers
6-16	1	18.4	55	4.8	269	Both towers
6-17	2	19.7	57	3.9	265	Tower 7-1 only
6-18	5	16.9	63	7.1	241	Tower 7-1 only
6-20	8	13.5	85	7.6	242	Tower 7-2 only
6-21	4	18.3	65	5.7	246	Tower 7-2 only
6-22	6	16.8	66	6.4	248	Both towers
6-24	7	16.7	61	7.7	248	Tower 7-1 only
6-25	x	15.9	65	5.4	268	Tower 7-1 only

Table 3-2

TABLE 3. Pittsburg plant source measurements summary of SP drift emission results [Source: (2)]

June 78 Date	Tower/ Cell	PreTest Rank	Total DME (gm/sec)	MMD (μm)	Ratio of IK-based DME to SP DME
15	1-7	Medium	2.59	73	6.2
16	1-12	Medium	4.57	785	4.0
17	1-3	High	6.76	721	2.2
18	1-9	Low	4.23	638	1.6
20	2-7	Medium	4.59	81.9	2.1
21	2-12	High	8.17	507	1.3
22	2-3	Medium	4.08	692	2.0

Legend: DME = drift mass emission
MMD = mass mean diameter

Table 3-3

Composite drift emission spectrum for each cell as a function of droplet size for the Pittsburg plant cooling towers [Source: (1)]

I	Drop Diameter/Interval d_ℓ (μm)	d_u (μm)	ΔDME/DME[1] (%)
1	10	20	0.5
2	20	30	4.4
3	30	40	7.4
4	40	50	6.5
5	50	60	5.5
6	60	70	3.5
7	70	90	3.3
8	90	110	1.8
9	110	130	0.9
10	130	150	0.8
11	150	180	1.1
12	180	210	1.2
13	210	240	1.3
14	240	270	1.4
15	270	300	1.8
16	300	350	2.7
17	350	400	2.3
18	400	450	2.3
19	450	500	1.5
20	500	600	4.3
21	600	700	3.5
22	700	800	3.8
23	800	900	2.7
24	900	1000	1.7
25	1000	1200	3.2
26	1200	1400	3.3
27	1400	1600	6.4
28	1600	1800	2.2
29	1800	2000	3.1
30	2000	2200	4.0
31	2200	2400	2.1
32	2400	2600	1.6
33	2600	2800	3.0
34	2800	3000	1.7
35	3000	3200	1.7
36	3200	3400	1.2
			99.7

Total Drift Mass Emission 4.76 gm/sec
Mass Median Diameter 492 μm

[1]The summation of this column is not 100.0% due to rounding

Table 3-4

Vertical ambient profile measurements
employed as input to ANL Model predictions

Date	Time(PST)	Height(m)	Temp(C°)	R.H.(%)	Wind Speed(ms^{-1})	Wind Direct.(°)
16 June	0858-	2	19.6	49.0	3.0	271
	0901	7	19.9	50.8	5.6	278
		25	18.6	51.4	5.5	241
		41	18.5	53.7	6.2	267
	0943-	12	20.9	40.4	6.6	224
	0948	22	20.6	50.4	6.2	244
		35	20.7	58.2	5.9	270
		52	20.6	57.0	5.9	269
	1034-	6	23.0	41.4	2.5	223
	1037	39	23.4	44.9	4.2	293
		60	21.2	50.1	6.2	302
		78	22.6	64.1	7.6	49
		108	22.1	59.9	4.7	271
17 June	0730-	9	18.0	65.2	2.4	276
	0744	18	17.8	65.7	2.3	299
		33	17.9	65.4	2.0	322
		58	17.6	67.3	2.2	338
		81	17.5	64.6	1.7	340
		100	17.6	60.7	1.3	17
	0829-	2	20.0	51.8	2.4	297
	0848	35	19.5	50.9	2.8	289
		45	19.3	45.8	2.6	303
		72	19.4	43.6	1.6	301
		95	19.1	43.9	1.1	278
		115	19.0	43.7	1.0	280
	0940-	16	21.0	56.1	5.1	323
	0943	39	21.4	53.7	4.9	294
		61	21.8	38.8	4.4	284
		106	22.1	34.4	3.5	272
	1047-	20	21.6	59.9	6.3	316
	1058	38	21.9	53.9	6.5	302
		57	23.0	34.6	5.4	298
		79	23.7	33.6	5.5	296
		95	23.1	32.5	5.1	295
	1129-	3	23.0	50.2	3.7	298
	1140	22	22.3	50.6	6.2	335
		47	22.7	38.6	7.2	304
		72	22.8	35.4	6.5	302
		95	22.9	37.4	5.2	301
		113	22.9	37.6	5.5	299

Table 3-4 continued

Date	Time(PST)	Height(m)	Temp(C°)	R.H.(%)	Wind Speed(ms^{-1})	Wind Direct.(°)
18 June	0900	10	16.8	63.0	7.0	236.7
	1000	10	17.9	60.0	7.0	240.0
	1100	10	19.4	55.7	7.0	245.0
	1200	10	20.7	52.7	7.5	253.3
	1300	10	21.8	50.0	7.7	256.7
21 June	0717-	4	14.7	77.7	6.3	253
	0729	22	14.7	76.4	5.7	267
		30	14.5	76.6	6.1	248
		43	14.3	77.7	5.9	256
		52	14.2	78.2	6.1	255
		76	14.0	78.7	6.0	254
		83	13.8	79.3	6.1	250
		91	13.8	80.1	6.4	244
		104	13.6	80.2	6.6	246
		112	13.5	80.7	6.3	253
	0850-	6	15.3	75.5	8.2	227
	0859	31	15.6	70.8	9.6	225
		55	15.5	71.1	8.5	242
		73	15.3	71.6	9.5	224
		90	15.2	72.2	9.1	233
		115	14.8	71.8	9.2	228
	0932-	4	18.5	64.2	6.4	232
	0942	35	17.0	66.9	7.7	238
		56	16.6	66.8	7.2	242
		73	16.4	67.7	7.2	250
		98	16.2	68.0	7.6	233
	1015-	7	18.6	61.9	5.3	226
	1023	20	18.4	62.4	7.5	233
		49	17.7	64.5	7.8	241
		74	17.6	64.8	6.8	244
		96	17.2	65.9	7.2	240
	1047-	5	19.9	56.5	5.6	229
	1055	30	19.3	59.6	6.7	246
		54	18.4	60.7	7.5	232
		65	18.4	60.2	7.3	217
		86	18.0	61.3	7.2	228
		112	17.8	62.3	6.4	233
	1149-	17	20.7	52.8	7.3	240
	1202	34	20.1	54.3	7.1	233
		43	19.9	55.0	7.1	249
		63	19.8	54.5	6.5	254
		78	19.9	54.2	6.9	238
		94	19.5	55.8	5.8	256
22 June	0900	10	16.8	67.3	6.8	247.5
	1000	10	18.5	60.4	6.8	245.0
	1100	10	20.7	55.2	6.3	246.4
	1200	10	22.4	49.1	6.3	252.4

Table 3-5

Sodium ion concentration and mineral ion concentration ratios of the Pittsburg unit 7 cooling tower circulating water [Source (1)].

	Basin/Canal Water Sodium Concentration[5] (mg/ℓ)				Mineral Ion Concentration Ratio[5]					
					$\frac{Mg^{++}}{Na^{+}}$		$\frac{Ca^{++2}}{Na^{+}}$	$\frac{K^{+2}}{Na^{+}}$	$\frac{C\ell^{-2}}{Na^{+}}$	$\frac{SO_4^{=2}}{Na^{+}}$
Date	ESC[1]	PNL[2]	ESC/PNL[3]	PG&E[4]	ESC[1]	PNL[2]				
6-13	--	--	--	57	--	--	--	--	--	--
6-15	96	102(10)	48	--	0.17	0.15(1)	0.17(1)	0.18(10)	1.11(5)	0.79(3)
6-16	105	132(26)	123	--	0.16	0.13(3)	0.14(3)	0.25(14)	1.27(47)	1.00(36)
6-17	125	140(43)	109	--	0.15	0.16(2)	0.15(3)	0.047(7)	1.63(31)	0.72(14)
6-18	204(30)	192(66)	244(34)	--	0.14	0.15(3)	0.12(3)	0.072(40)	1.67(36)	0.62(17)
6-20	275	296(30)	420	202	0.14	0.14(1)	0.10(1)	0.037(5)	1.74(24)	0.47(5)
6-21	--	450(75)	--	--	--	0.12(1)	0.074(8)	0.035(11)	1.68(29)	0.41(7)
6-22	466(30)	701(142)	963(87)	--	0.13	0.090(13)	0.053(8)	0.041(16)	1.26(16)	0.27(4)
6-24	--	653(167)	--	--	--	0.10(2)	0.063(12)	0.044(5)	1.46(17)	0.31(6)
				Average	0.15(2)	0.13(3)	0.11(4)	0.046(13)[6]	1.48(24)	0.57(25)

[1]ESC analysis of ESC samples.
[2]PNL analysis of PNL samples.
[3]PNL analysis of ESC samples.
[4]Calculated by ESC from PG&E analysis, assuming Na^{+} is 34% of salts in seawater.
[5]Shorthand notation for standard deviation, e.g., 204(30) = 204 ± 30, 0.51(1) = 0.51 ± 0.01
[6]Averaged w/o 6-15 and 6-16.

Table 3-6

Downwind sampling station identification and location relative to both cooling towers [Source:(1)]

(θ = 0° = North)

Station ID	Tower 7-1 R_1 (m)	Tower 7-1 θ_1 (°)	Tower 7-2 R_2 (m)	Tower 7-2 θ_2 (°)
UUA	821	278	500	280
UUB	825	269	500	265
UA	566	280	250	290
UB	573	267	250	260
OA	125	310	245	69
OBN	110	275	216	86
OBS	110	256	219	95
OC	115	230	246	106
OD	170	220	249	120
OE	250	220	248	139
1X	160	6	379	64
1ZZ	135	20	394	70
1Z	230	37	501	68
1Y	230	53	529	74
1A	215	64	528	79
1B	215	77	537	84
1C	215	92	540	90
1D	225	105	545	96
1E	255	120	559	103
1F	275	130	562	108
1G	300	144	555	115
1I	235	163	451	119
1J	275	178	429	129
1AZ	320	62	627	76
1AA	305	72	623	81
1AB	270	84	594	87
1AC	285	90	610	89
1AD	305	105	624	97
1AE	325	116	632	103
1AF	375	111	687	101

Station ID	Tower 7-1 R_1 (m)	Tower 7-1 θ_1 (°)	Tower 7-2 R_2 (m)	Tower 7-2 θ_2 (°)
2A	420	60	722	73
2B	420	68	733	77
2E	560	95	884	93
2F	550	101	871	97
2G	595	110	906	103
2H	625	120	919	110
2I	605	132	871	117
2J	505	144	741	123
2K	480	158	664	131
3A	695	86	1020	87
3B	750	94	1074	92
3C	775	101	1095	97
3E	765	119	1059	110
3F	745	124	1028	114
Tower 7-2	325	269	-	-
Tower 7-1	-	-	325	89

Table 3-7

Comparison of ANL Model predictions of sodium deposition rate and field data for the survey date of June 16 at Pittsburg, California

Arc 0

SAMPLER	OBSERVED SODIUM DEPOSITION RATE ($\mu g/(m^2 - hr)$)	ANL-PREDICTED SODIUM DEPOSITION RATE ($\mu g/(m^2 - hr)$)
0A	3	11.1
0BN	112	32.5
0BS	31	32.4
0D	192	8.5
0E	0	3.2

Arc 1

SAMPLER	OBSERVED SODIUM DEPOSITION RATE ($\mu g/(m^2 - hr)$)	ANL-PREDICTED SODIUM DEPOSITION RATE ($\mu g/(m^2 - hr)$)
1A	0	13.6
1B	5	24.1
1C	125, 194	30.1
1D	41, 52	20.5
1E	0	6.1
1F	31, 22	3.3
1G	16	1.6
1I	0	4.0
1J	0	3.7

Table 3-7 continued

Arc 2

SAMPLER	OBSERVED SODIUM DEPOSITION RATE ($\mu g/(m^2 - hr)$)	ANL-PREDICTED SODIUM DEPOSITION RATE ($\mu g/(m^2 - hr)$)
2A	0	0.9
2B	0	0.9
2E	7	0.0
2F	1.5, 0	0.0
2G	0	0.0
2H	5, 36	0.0
2I	7	0.0
2J	3	0.8
2K	0	0.5

Arc 3

SAMPLER	OBSERVED SODIUM DEPOSITION RATE ($\mu g/(m^2 - hr)$)	ANL-PREDICTED SODIUM DEPOSITION RATE ($\mu g/(m^2 - hr)$)
3A	14	0.0
3B	9	0.0
3C	23	0.0
3E	23, 67	0.0
3F	0	0.0

Table 3-8

Comparison of ANL Model predictions of sodium deposition rate and field data for the survey date of June 17 at Pittsburg, California.

Arc 1

SAMPLER	OBSERVED SODIUM DEPOSITION RATE ($\mu g/(m^2 - hr)$)	ANL-PREDICTED SODIUM DEPOSITION RATE ($\mu g/(m^2 - hr)$)
1C	0	10.9
1D	$\begin{matrix}41\\38\end{matrix}$]	21.5
1E	18	27.3
1F	0	26.8

Arc 1A

SAMPLER	OBSERVED SODIUM DEPOSITION RATE ($\mu g/(m^2 - hr)$)	ANL-PREDICTED SODIUM DEPOSITION RATE ($\mu g/(m^2 - hr)$)
1AA	56	0.9
1AB	23	1.2
1AC	$\begin{matrix}0\\4\end{matrix}$]	1.9
1AD	$\begin{matrix}34\\59\end{matrix}$]	7.6
1AF	8	13.3

Arc 2

SAMPLER	OBSERVED SODIUM DEPOSITION RATE ($\mu g/(m^2 - hr)$)	ANL-PREDICTED SODIUM DEPOSITION RATE ($\mu g/(m^2 - hr)$)
2E	1	0.14
2F	$\begin{matrix}0\\17\end{matrix}$]	0.41
2G	$\begin{matrix}0\\3\end{matrix}$]	0.10
2H	0	0.05

Arc 3

SAMPLER	OBSERVED SODIUM DEPOSITION RATE ($\mu g/(m^2 - hr)$)	ANL-PREDICTED SODIUM DEPOSITION RATE ($\mu g/(m^2 - hr)$)
3C	9	0.003
3E	15	0.006

Table 3-9

Comparison of ANL Model predictions of sodium deposition rate and field data for the survey date of June 18 at Pittsburg, California.

Arc 1

SAMPLER	OBSERVED SODIUM DEPOSITION RATE ($\mu g/(m^2 - hr)$)	ANL-PREDICTED SODIUM DEPOSITION RATE ($\mu g/(m^2 - hr)$)
1Z	$\frac{9}{45}$]	22.2
1Y	46	88.5
1A	$\frac{42}{76}$]	186.7
1B	119	199.7
1C	$\frac{199}{106}$]	45.2

Arc 1A

SAMPLER	OBSERVED SODIUM DEPOSITION RATE ($\mu g/(m^2 - hr)$)	ANL-PREDICTED SODIUM DEPOSITION RATE ($\mu g/(m^2 - hr)$)
1AZ	5	20.7
1AA	$\frac{77}{92}$]	43.9
1AB	40	27.4
1AC	71	8.3

Arc Z

SAMPLER	OBSERVED SODIUM DEPOSITION RATE ($\mu g/(m^2 - hr)$)	ANL-PREDICTED SODIUM DEPOSITION RATE ($\mu g/(m^2 - hr)$)
2A	2	6.1
2B	$\frac{18}{14}$]	6.7

Table 3-10

Comparison of ANL Model prediction of sodium deposition rate and field data for the survey date of June 21 at Pittsburg, California

Arc 0

SAMPLER	OBSERVED SODIUM DEPOSITION RATE ($\mu g/(m^2 - hr)$)	ANL-PREDICTED SODIUM DEPOSITION RATE ($\mu g/(m^2 - hr)$)
0A	142, 123	477.1
0BN	148	92.6
0BS	47	47.2
0C	11	18.5

Arc 1

SAMPLER	OBSERVED SODIUM DEPOSITION RATE ($\mu g/(m^2 - hr)$)	ANL-PREDICTED SODIUM DEPOSITION RATE ($\mu g/(m^2 - hr)$)
1ZZ	240	25.0
1Z	0	8.0
1Y	12, 30	5.4
1A	23, 11	4.6
1B	118, 20	3.5
1C	188	2.4

Arc 1A

SAMPLER	OBSERVED SODIUM DEPOSITION RATE ($\mu g/(m^2 - hr)$)	ANL-PREDICTED SODIUM DEPOSITION RATE ($\mu g/(m^2 - hr)$)
1AZ	75, 44	0.71
1AA	12	0.58
1AB	1, 131	0.79
1AC	33	0.48

Arc 2

SAMPLER	OBSERVED SODIUM DEPOSITION RATE ($\mu g/(m^2 - hr)$)	ANL-PREDICTED SODIUM DEPOSITION RATE ($\mu g/(m^2 - hr)$)
2A	0	0.1
2B	89	0.006

Table 3-11

Comparison of ANL Model prediction of sodium deposition rate and field data for the survey date of June 22 at Pittsburg, California

Arc 0

SAMPLER	OBSERVED SODIUM DEPOSITION RATE ($\mu g/(m^2 - hr)$)	ANL-PREDICTED SODIUM DEPOSITION RATE ($\mu g/(m^2 - hr)$)
0A	89, 113	537.5
0BN	176, 116	453.9
0BS	13	85.6
0C	13	26.2

Arc 1

SAMPLER	OBSERVED SODIUM DEPOSITION RATE ($\mu g/(m^2 - hr)$)	ANL-PREDICTED SODIUM DEPOSITION RATE ($\mu g/(m^2 - hr)$)
1ZZ	78	107.5
1Z	0	60.6
1Y	100	242.0
1A	113, 179	584.6
1B	273	792.4
1C	141, 228	117.2

Arc 1A

SAMPLER	OBSERVED SODIUM DEPOSITION RATE ($\mu g/(m^2 - hr)$)	ANL-PREDICTED SODIUM DEPOSITION RATE ($\mu g/(m^2 - hr)$)
1AZ	78, 110	47.7
1AA	267	68.3
1AB	84	74.3
1AC	53, .7	47.6

Arc 2

SAMPLER	OBSERVED SODIUM DEPOSITION RATE ($\mu g/(m^2 - hr)$)	ANL-PREDICTED SODIUM DEPOSITION RATE ($\mu g/(m^2 - hr)$)
2A	0	11.1
2B	102, 20	12.8

Table 3-12

Statistical results of ANL Model predictions

Case	N5	N3	N2	$\emptyset_o$	$\emptyset_p$	# samplers
PITT 16	7	2	2	10	10	28
PITT 17	7	6	6	3	0	15
PITT 18	10	8	5	0	0	11
PITT 21	7	6	4	2	0	16
PITT 22	13	9	6	2	0	16

where

N5 = number of model predictions within a factor of 5
N3 = number of model predictions within a factor of 3
N2 = number of model predictions within a factor of 2
$\emptyset_o$ = number of samplers with 0 observed sodium deposition
$\emptyset_p$ = number of samplers where model predicts 0 sodium deposition

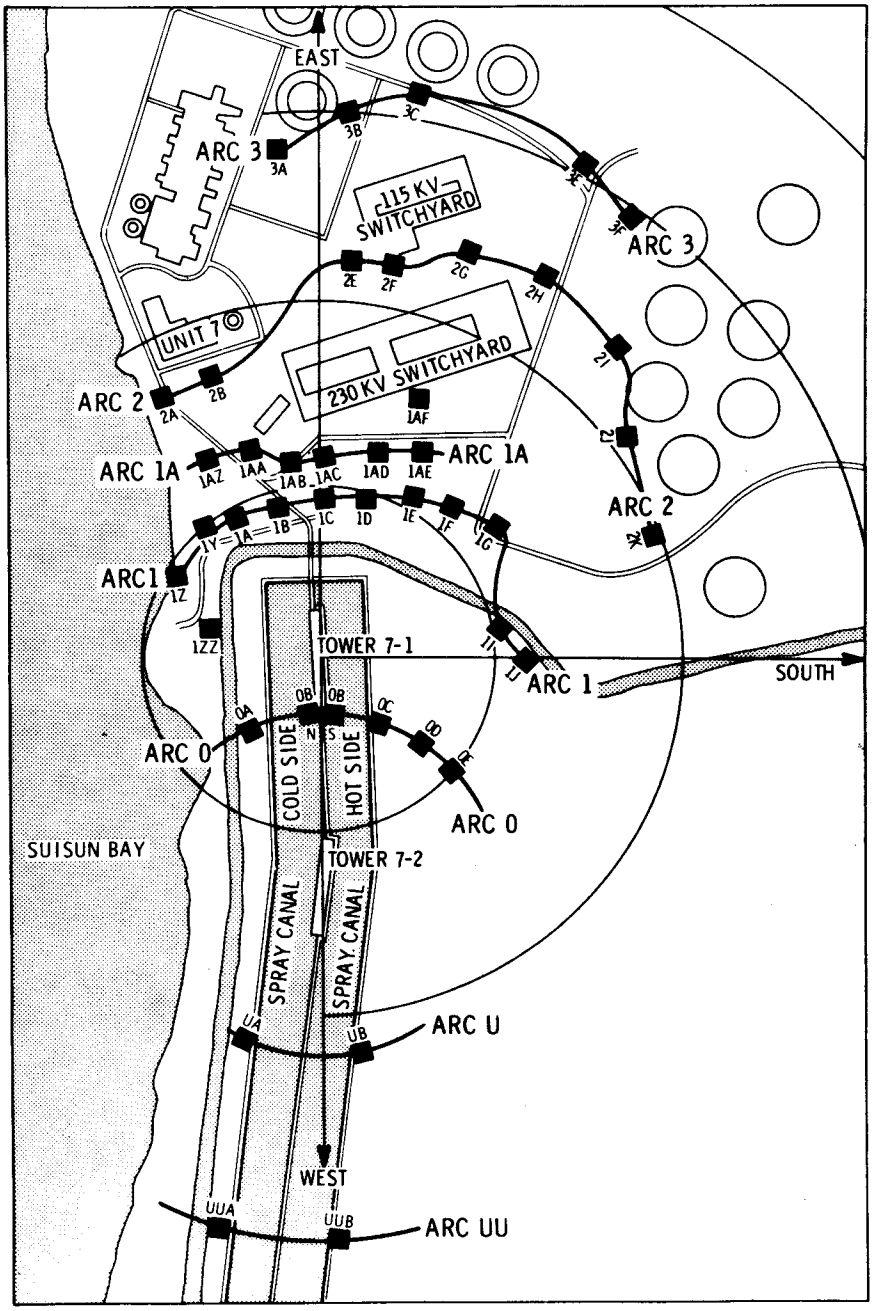

Figure 3-1. Sampling station and plant layout for the Pittsburg power plant cooling tower drift study [Source: (1)].

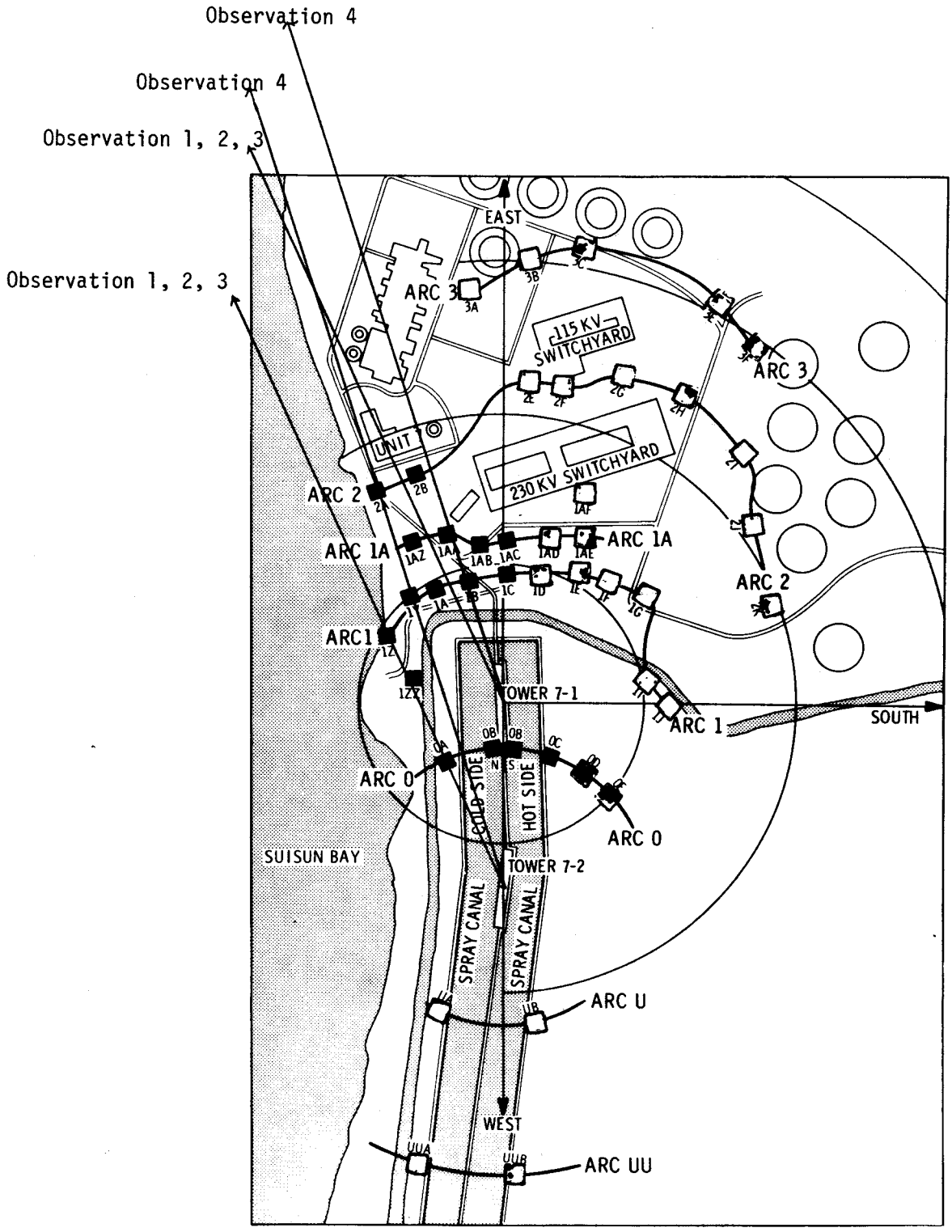

Figure 3-10. Operating sampler stations and observed wind direction for the Pittsburg power plant cooling tower drift experiment of June 22, 1978.

legend. [Source: (1)].

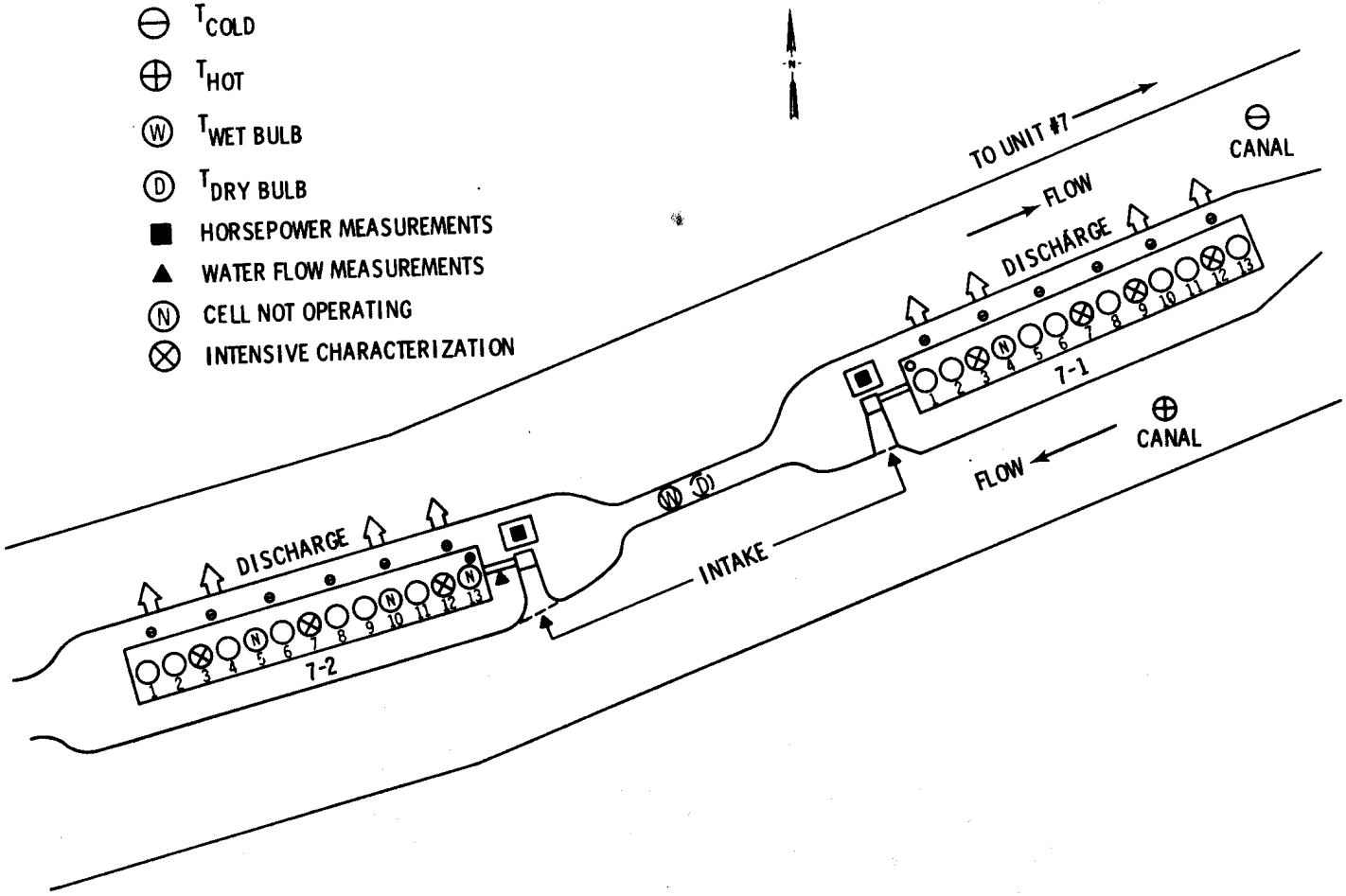

Figure 3-2. Cooling tower layout, cell designation and identification of cells selected for intensive characterization. Measurement location of cooling tower parameters are also shown and identified in the

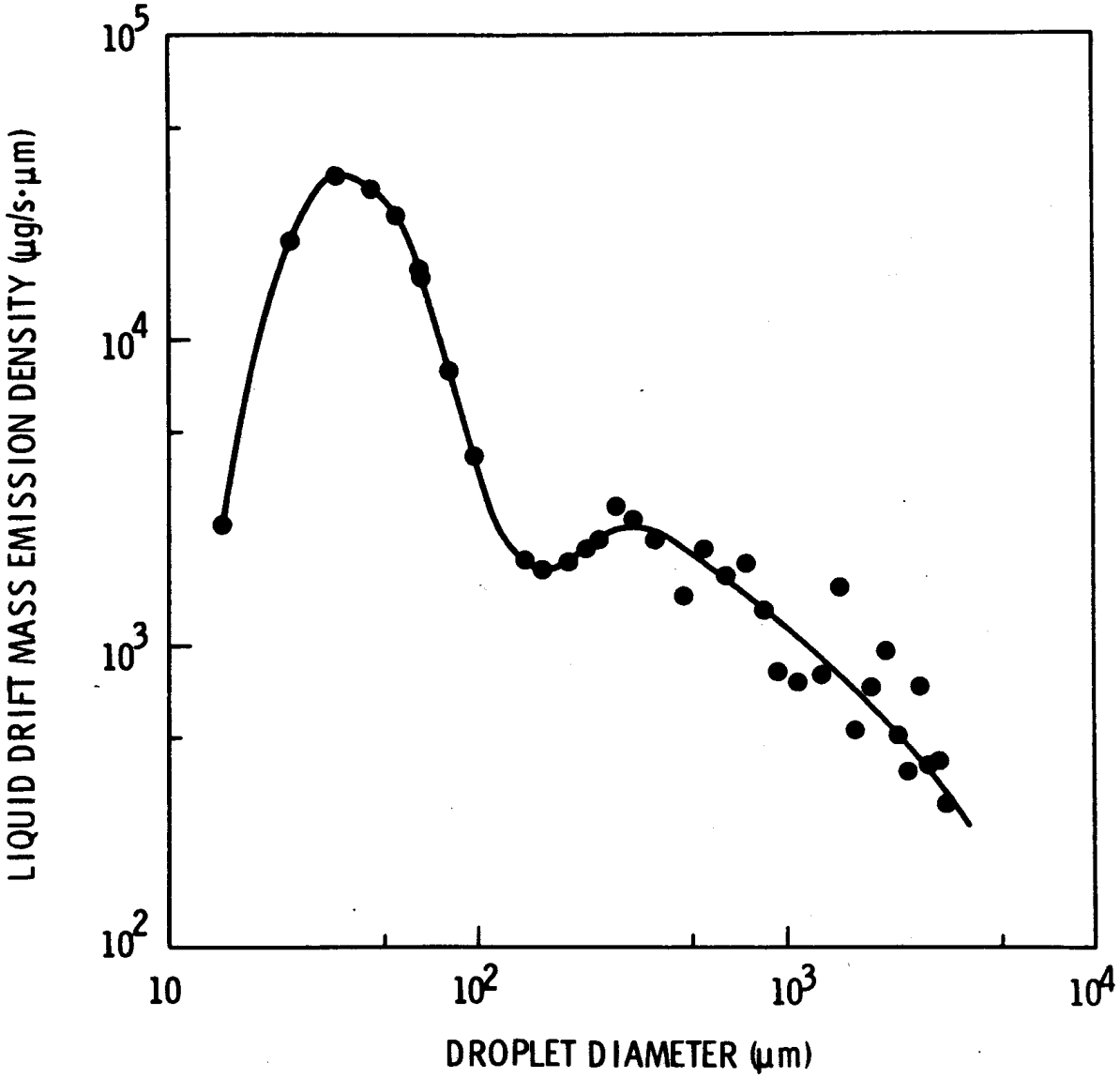

Figure 3-3. Composite drift mass emission spectrum for all cells for the Pittsburg cooling towers. [Source: (1)].

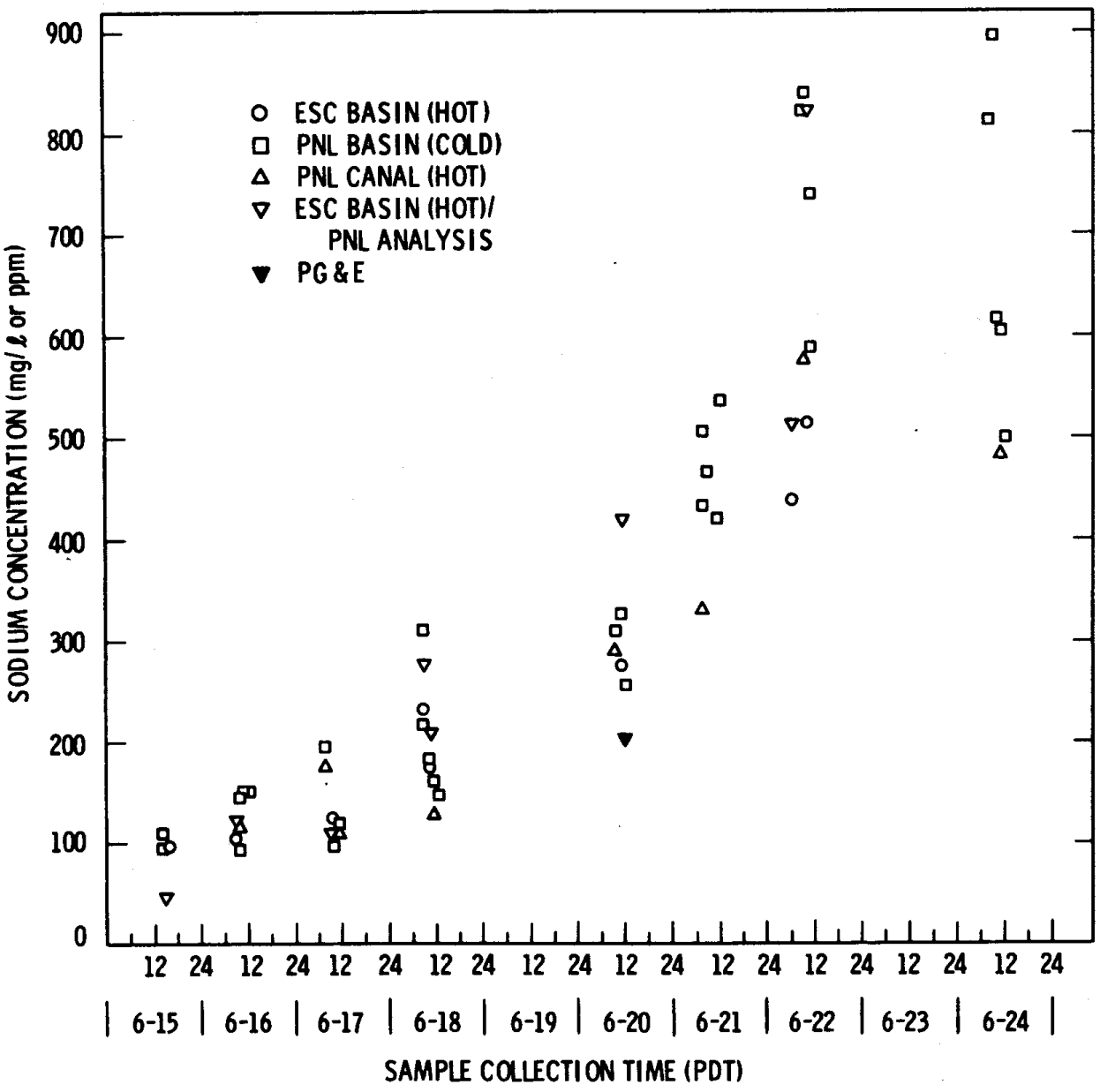

Figure 3-4. Sodium ion concentration of the cooling tower circulating water as a function of sample collection time and day. The PG&E value is calculated from a total salt concentration assuming that Na^+ is 34% of the salts in seawater. [Source: (1)].

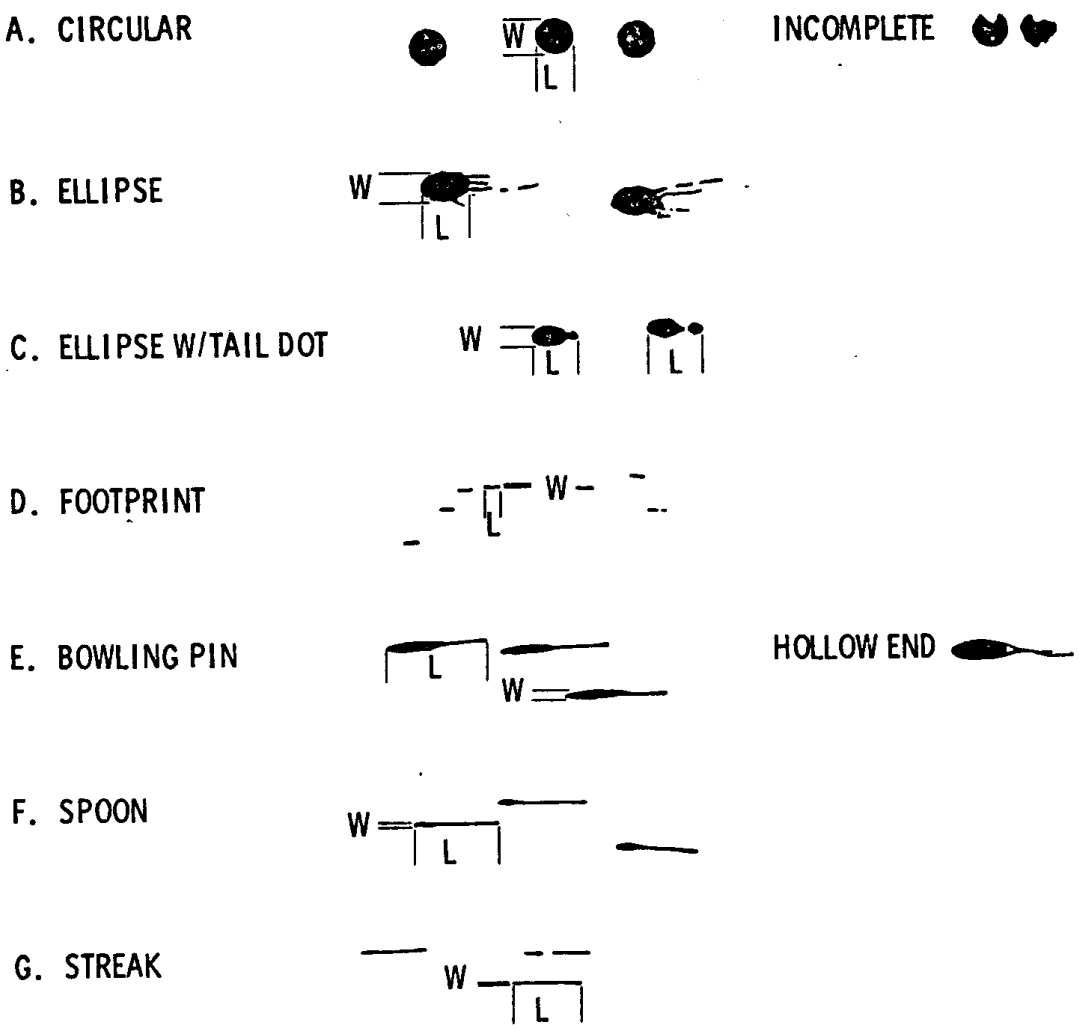

Figure 3-5. ESC Stain Shape Classification for measured droplet deposition at Pittsburg, California. [Source: (1)].

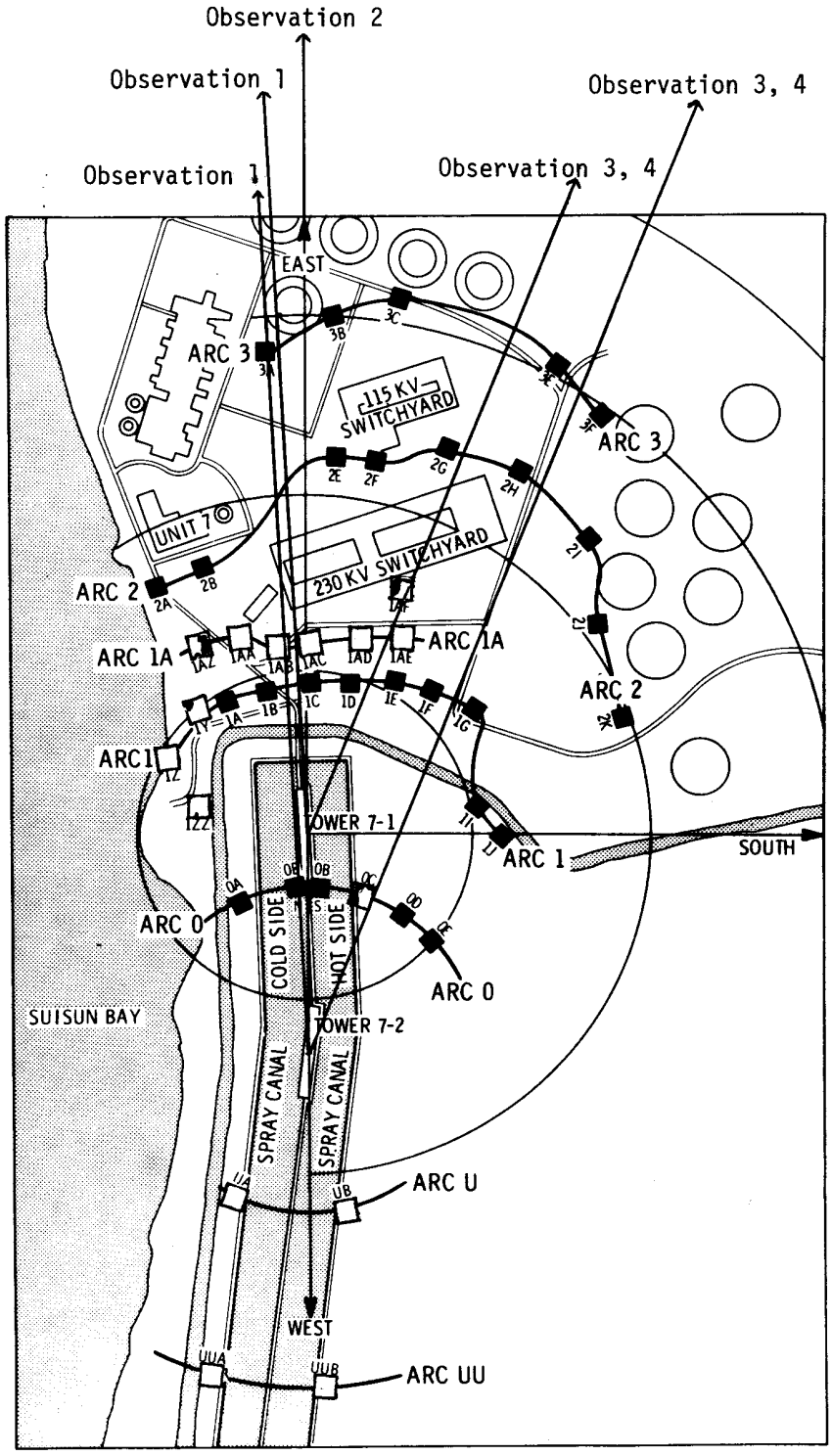

Figure 3-6. Operating sampler stations and observed wind direction for the Pittsburg power plant cooling tower drift experiment of June 16, 1978.

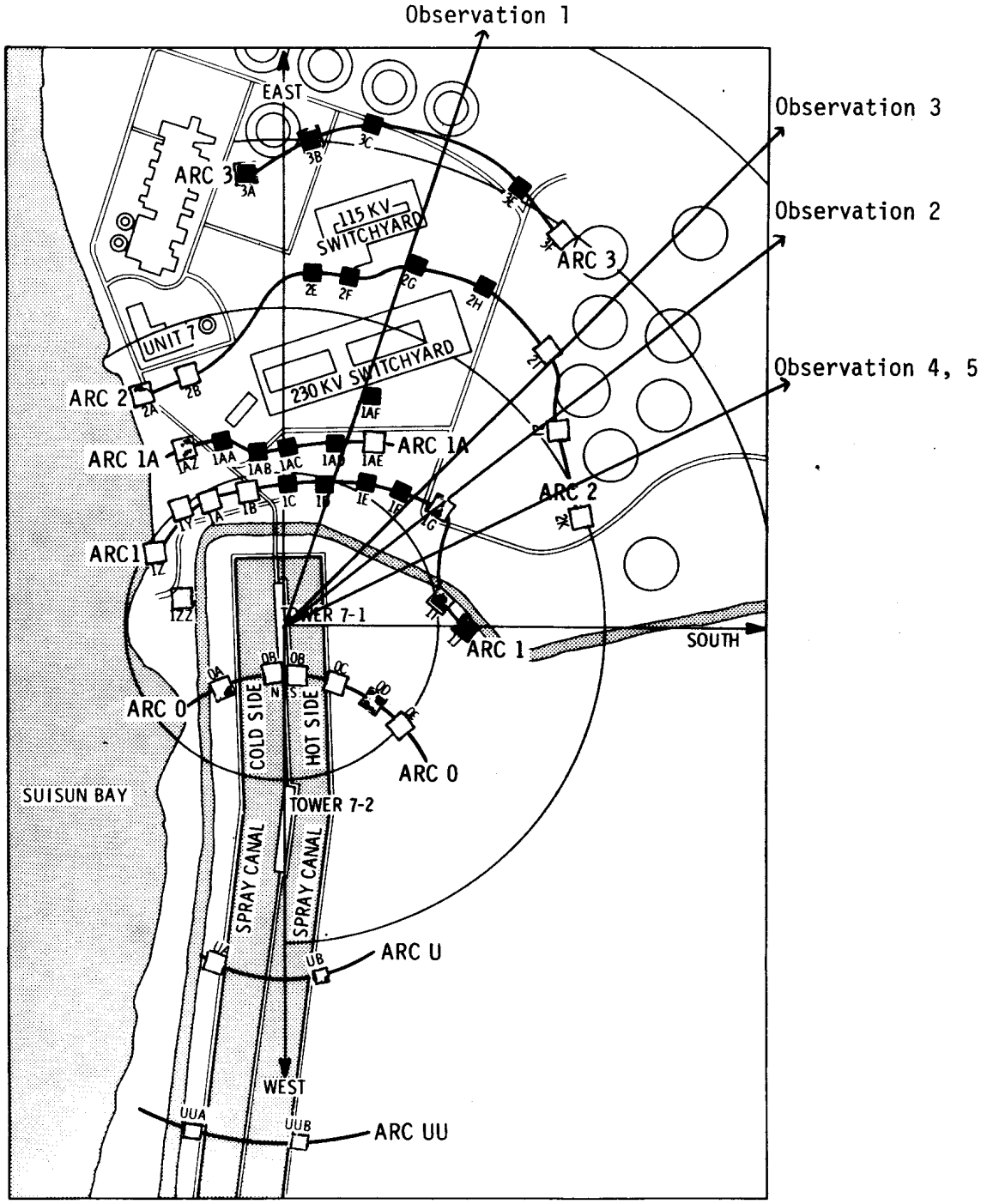

Figure 3-7. Operating sampler stations and observed wind direction for the Pittsburg power plant cooling tower drift experiment of June 17, 1978.

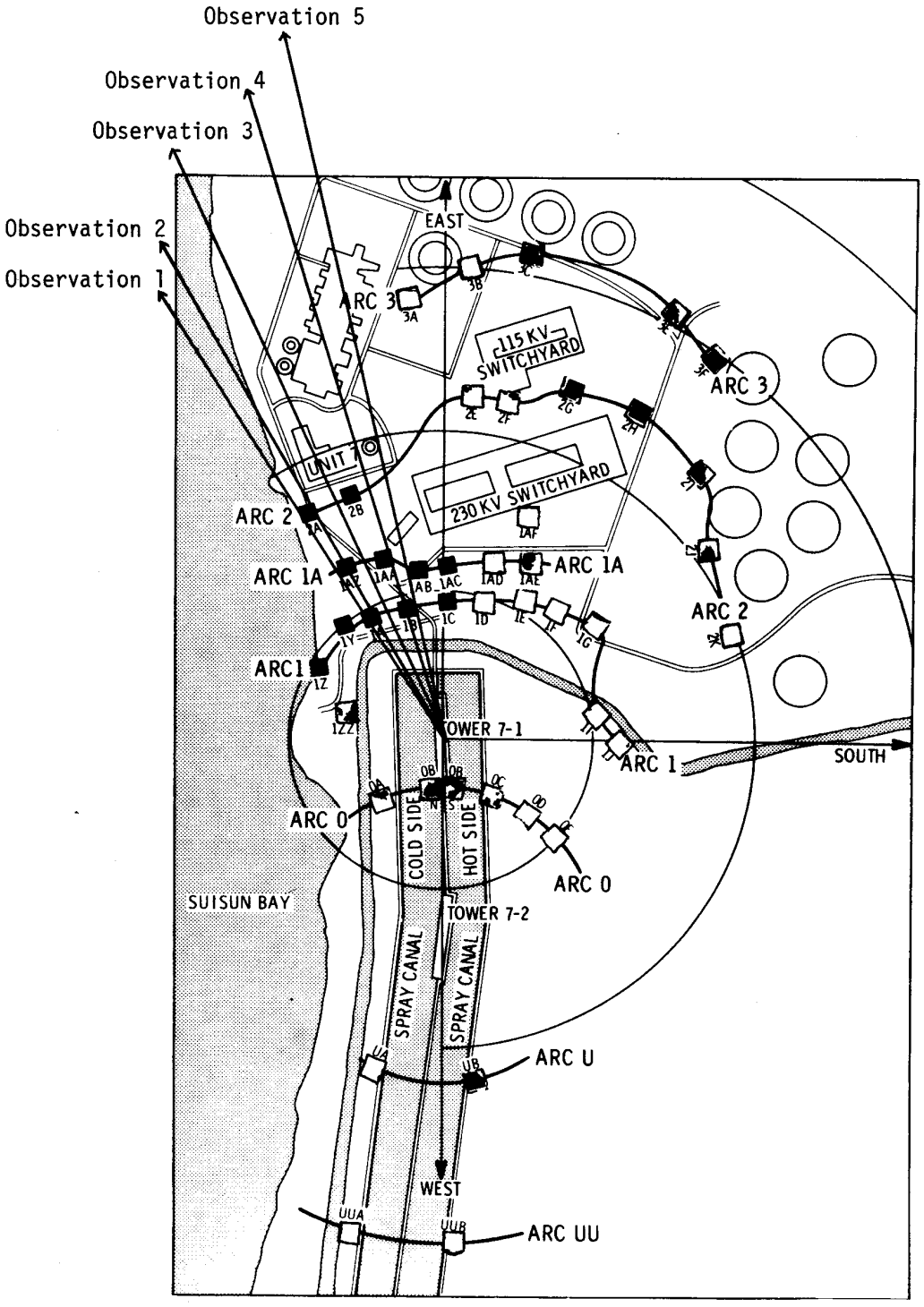

Figure 3-8. Operating sampler stations and observed wind direction for the Pittsburg power plant cooling tower drift experiment of June 18, 1978.

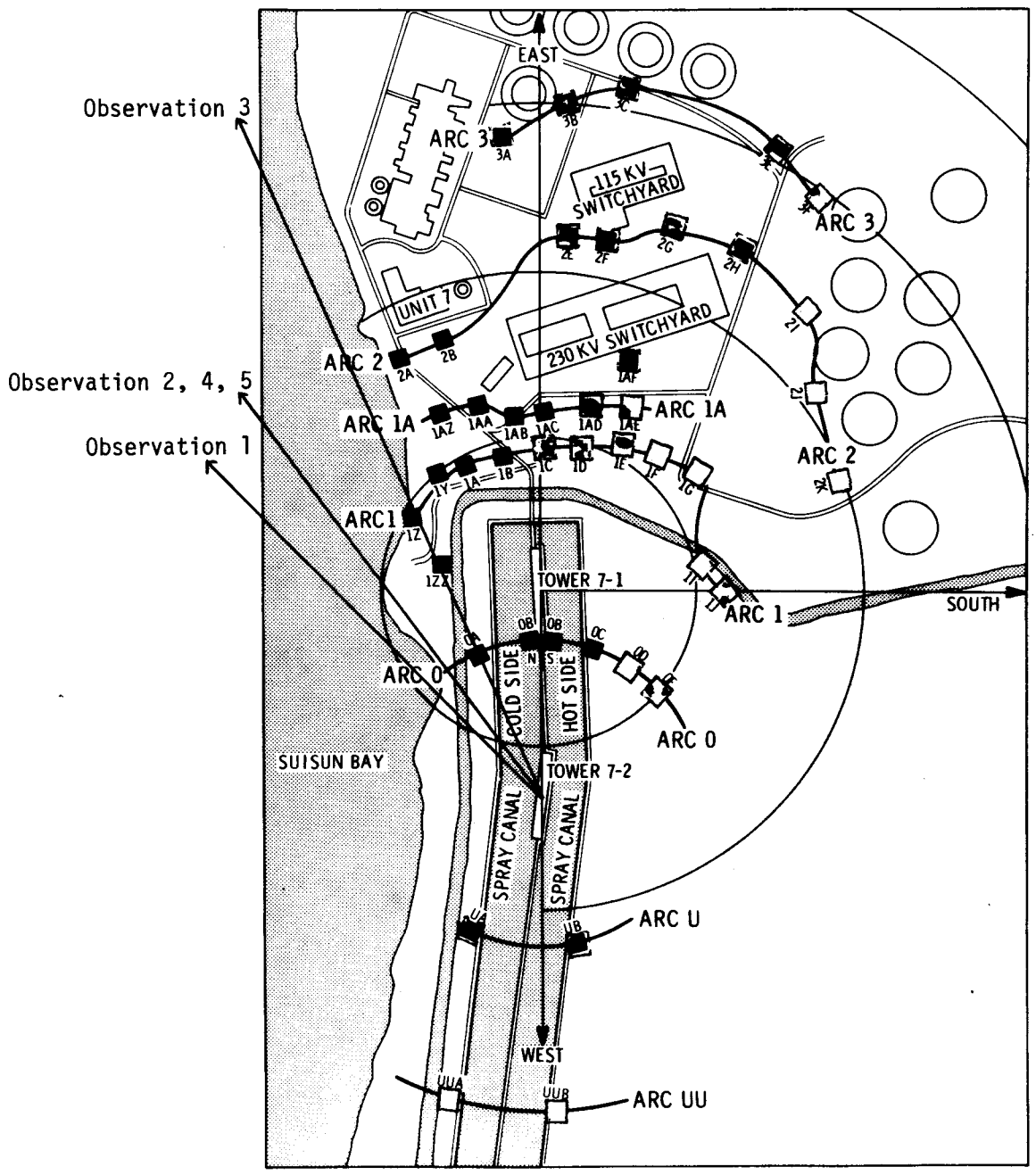

Figure 3-9. Operating sampler stations and observed wind direction for the Pittsburg power plant cooling tower drift experiment of June 21, 1978.

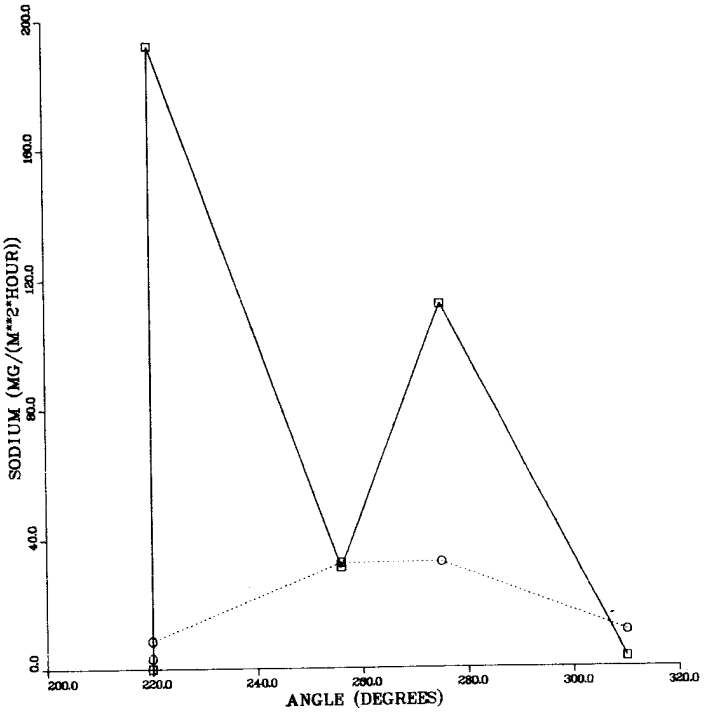

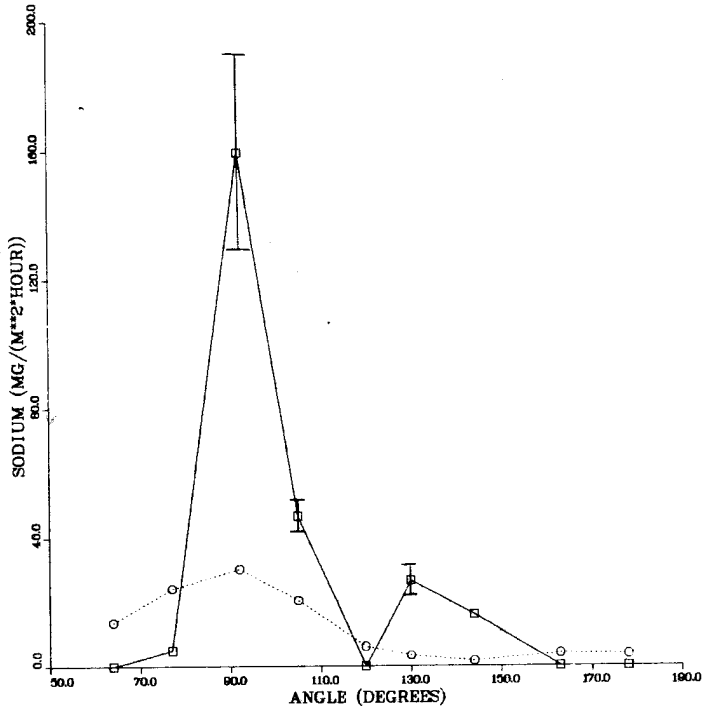

Figure 3-11. Comparison of ANL predicted and observed sodium deposition rate for Pittsburg California drift study of June 16, 1978.

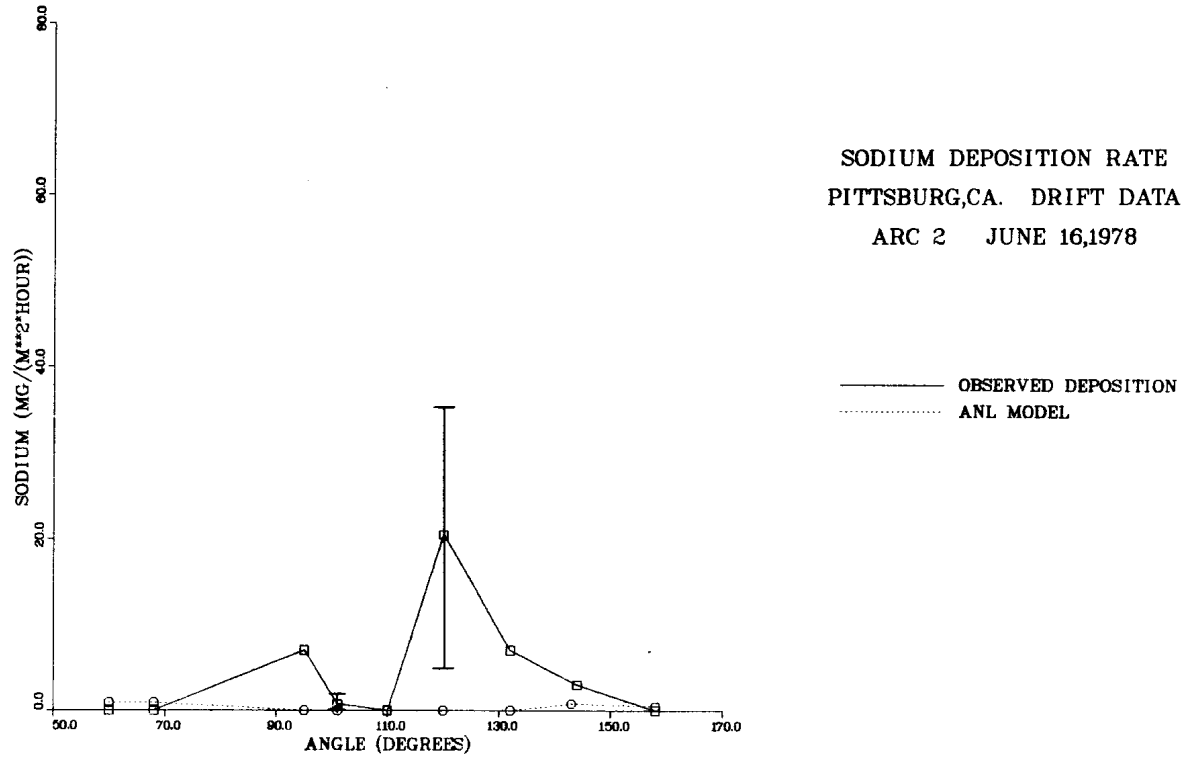

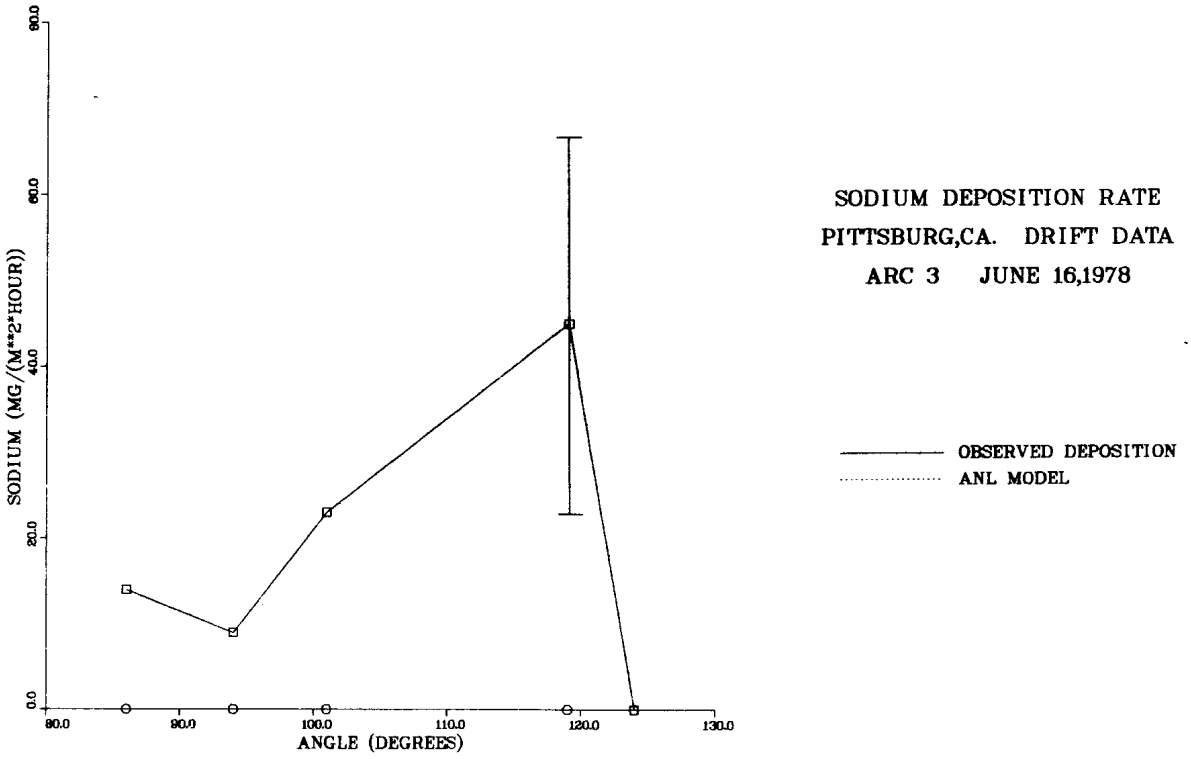

Figure 3-12. Comparison of ANL predicted and observed sodium deposition rate for Pittsburg California drift study of June 16, 1978.

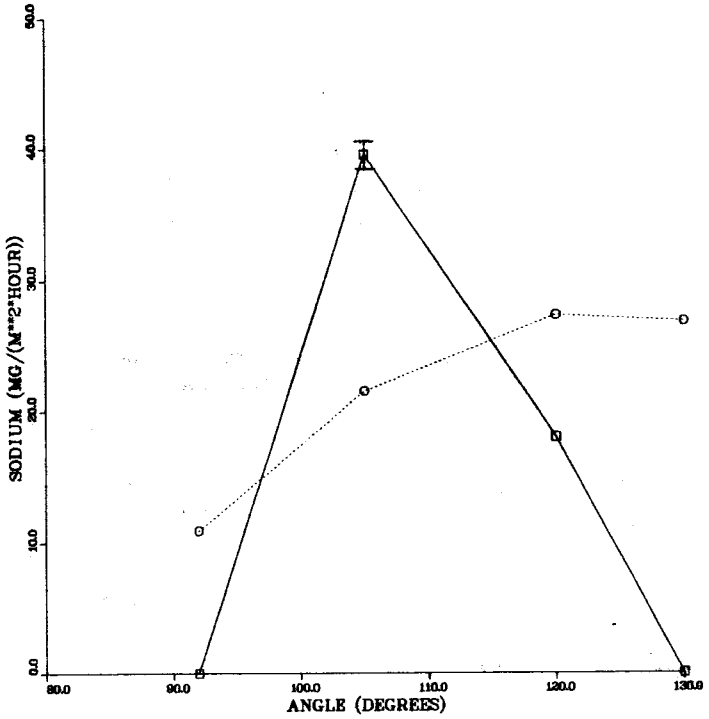

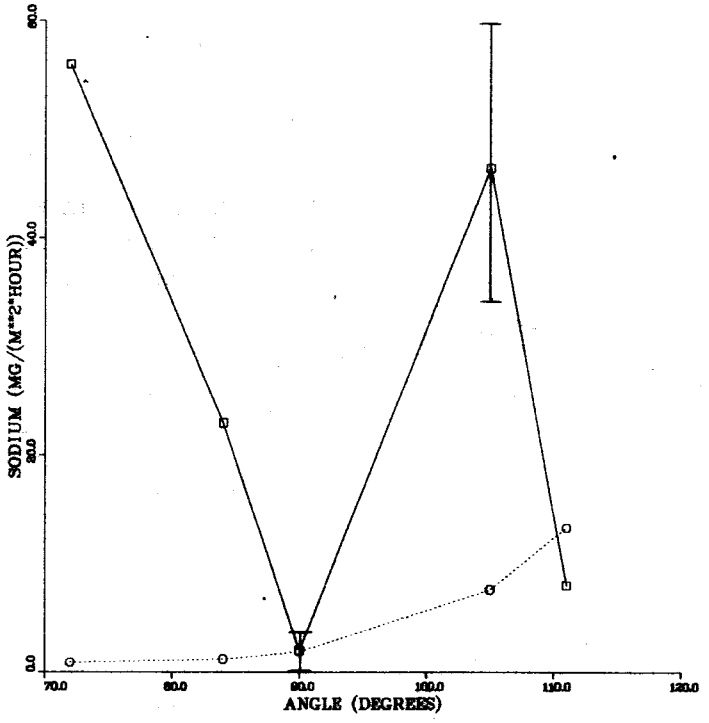

Figure 3-13. Comparison of ANL predicted and observed sodium deposition rate for Pittsburg California drift study of June 17, 1978.

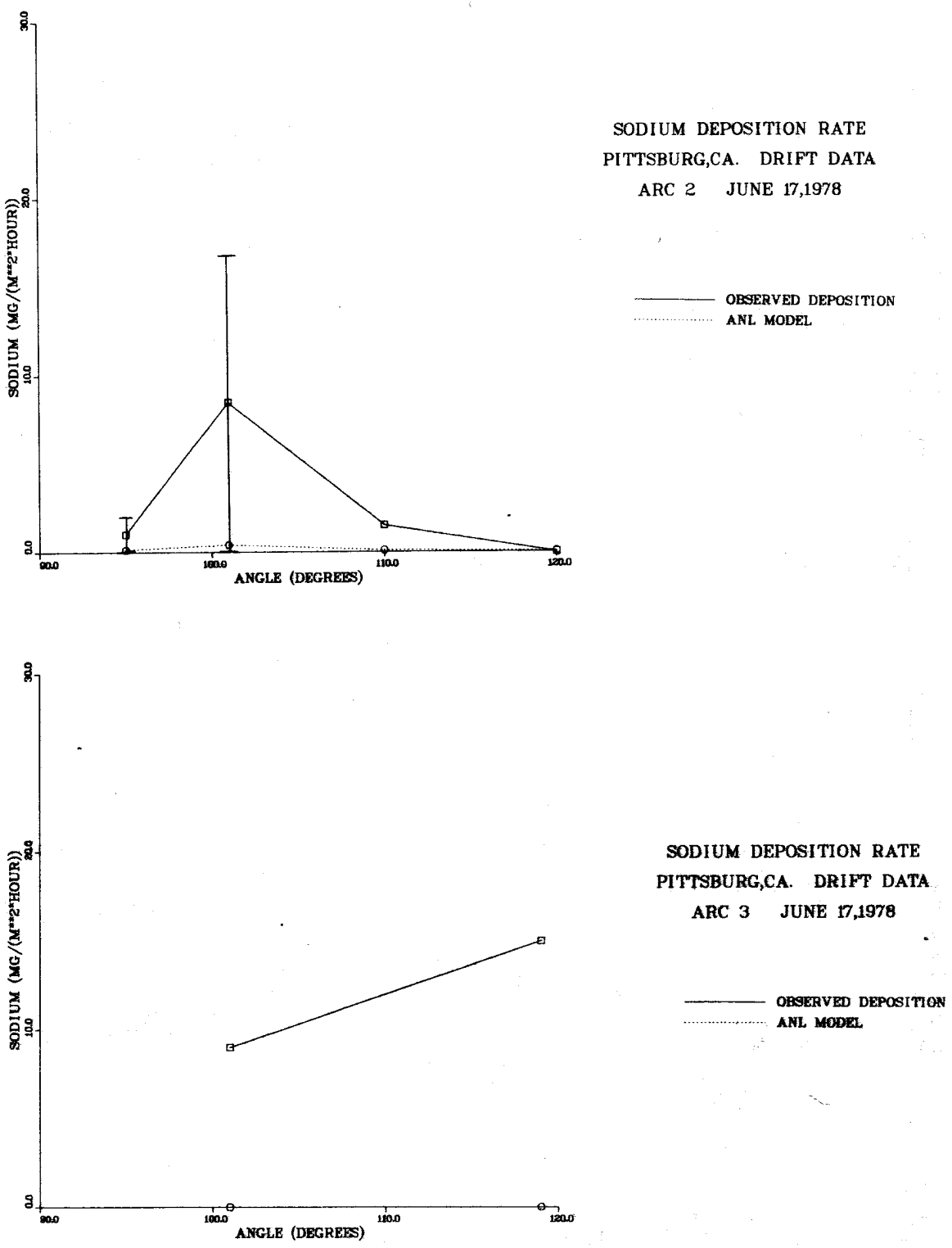

Figure 3-14. Comparison of ANL predicted and observed sodium deposition rate for Pittsburg California drift study of June 17, 1978.

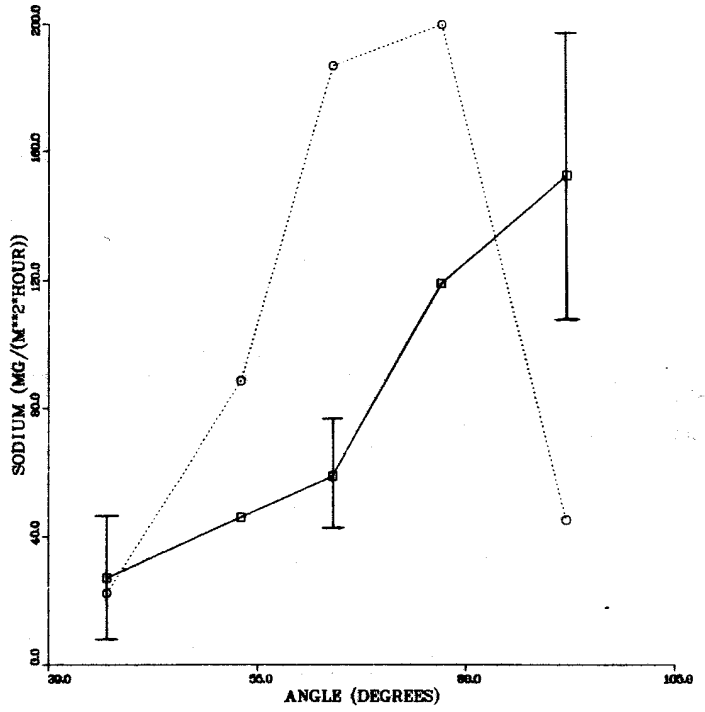

SODIUM DEPOSITION RATE
PITTSBURG,CA. DRIFT DATA
ARC 1 JUNE 18,1978

OBSERVED DEPOSITION
ANL MODEL

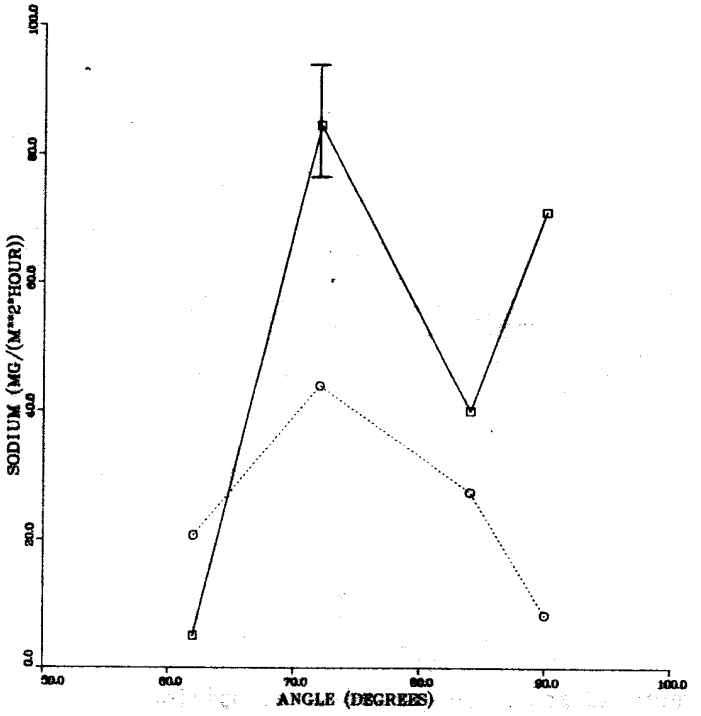

SODIUM DEPOSITION RATE
PITTSBURG,CA. DRIFT DATA
ARC 1A JUNE 18,1978

OBSERVED DEPOSITION
ANL MODEL

Figure 3-15. Comparison of ANL predicted and observed sodium deposition rate for Pittsburg California drift study of June 18, 1978.

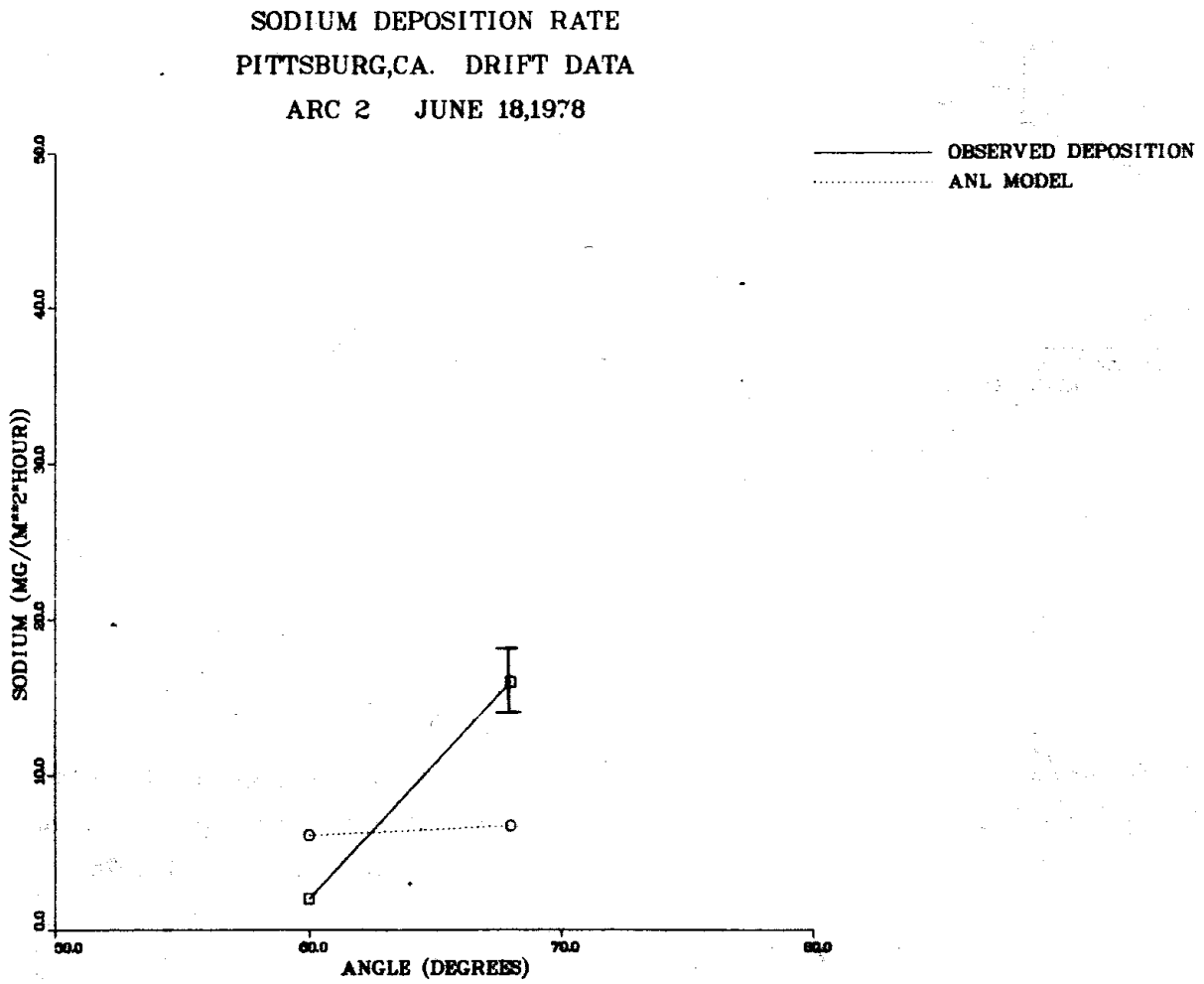

Figure 3-16. Comparison of ANL predicted and observed sodium deposition rate for Pittsburg California drift study of June 18, 1978.

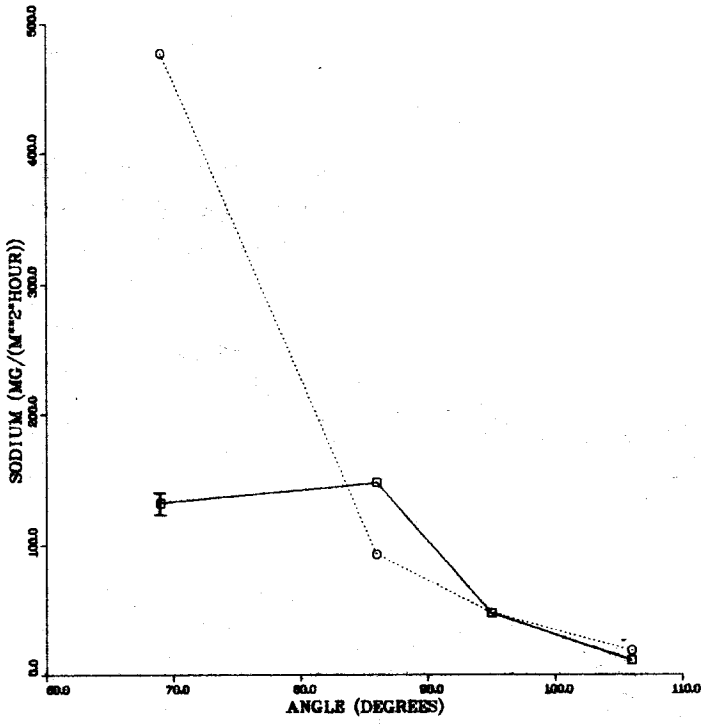

SODIUM DEPOSITION RATE
PITTSBURG,CA. DRIFT DATA
ARC 0 JUNE 21,1978

OBSERVED DEPOSITION
ANL MODEL

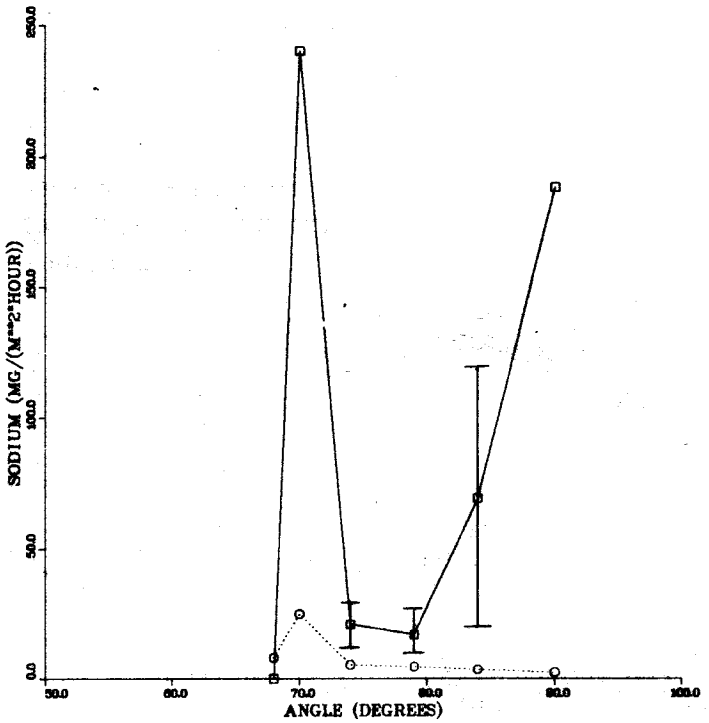

SODIUM DEPOSITION RATE
PITTSBURG, CA. DRIFT DATA
ARC 1 JUNE 21, 1978

OBSERVED DEPOSITION
ANL MODEL

Figure 3-17. Comparison of ANL predicted and observed sodium deposition rate for Pittsburg California drift study of June 21, 1978.

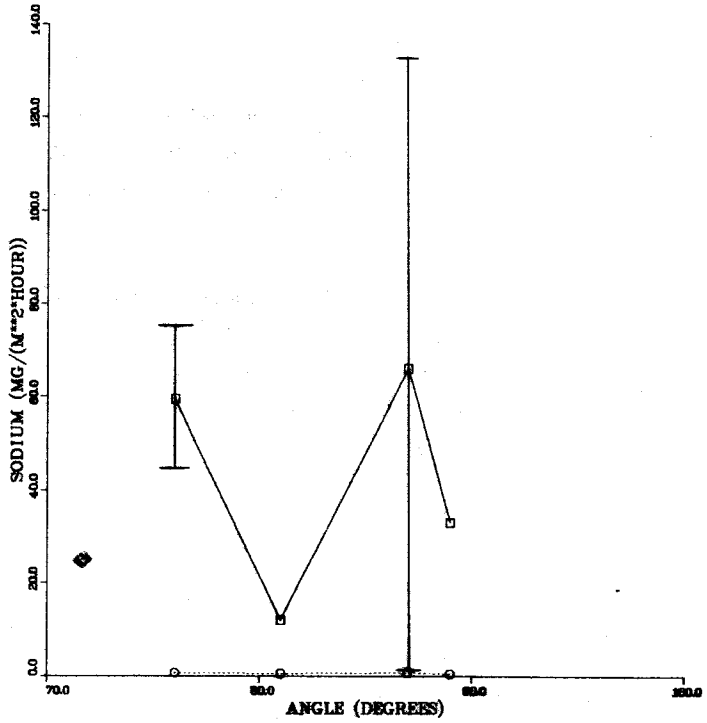

SODIUM DEPOSITION RATE
PITTSBURG,CA. DRIFT DATA
ARC 1A JUNE 21,1978

OBSERVED DEPOSITION
ANL MODEL

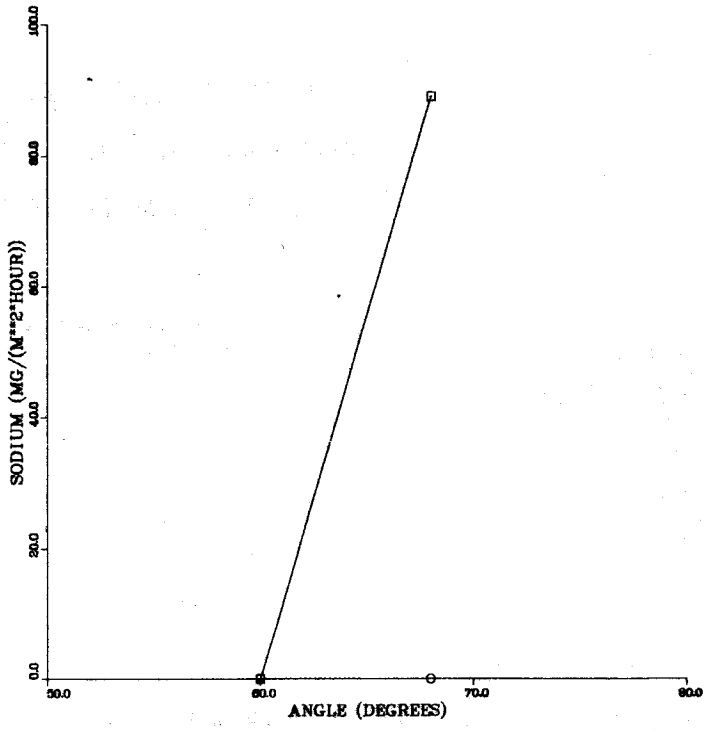

SODIUM DEPOSITION RATE
PITTSBURG,CA. DRIFT DATA
ARC 2 JUNE 21,1978

OBSERVED DEPOSITION
ANL MODEL

Figure 3-18. Comparison of ANL predicted and observed sodium deposition rate for Pittsburg California drift study of June 21, 1978.

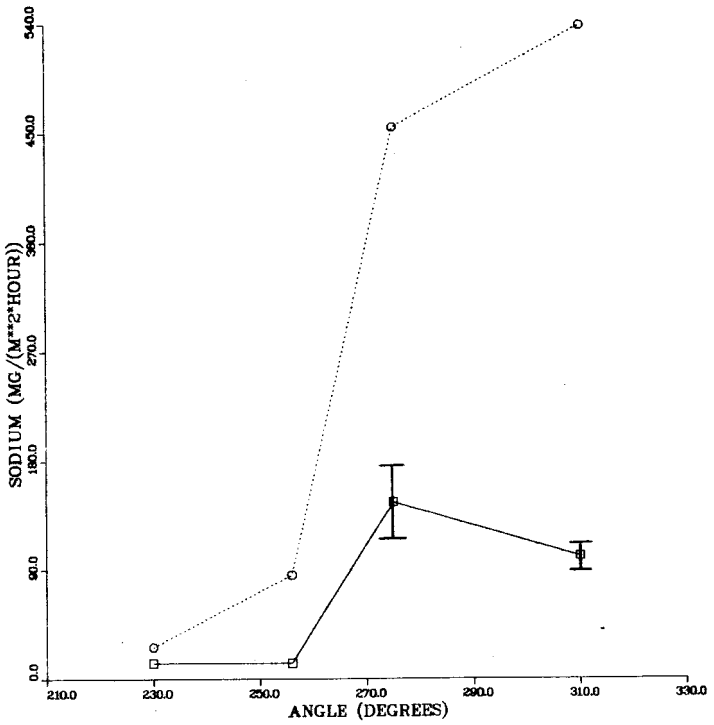

SODIUM DEPOSITION RATE
PITTSBURG,CA. DRIFT DATA
ARC 0 JUNE 22,1978

OBSERVED DEPOSITION
ANL MODEL

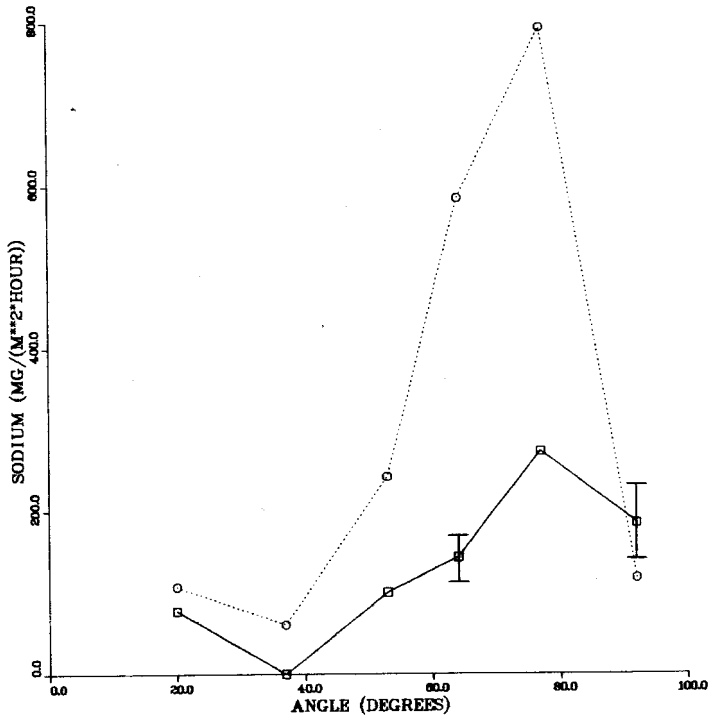

SODIUM DEPOSITION RATE
PITTSBURG,CA. DRIFT DATA
ARC 1 JUNE 22,1978

OBSERVED DEPOSITION
ANL MODEL

Figure 3-19. Comparison of ANL predicted and observed sodium deposition rate for Pittsburg California drift study of June 22, 1978.

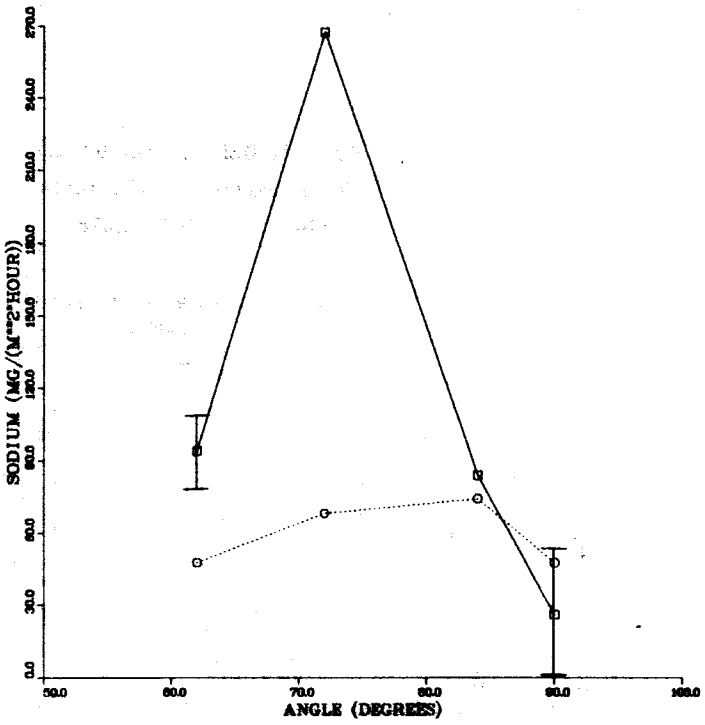

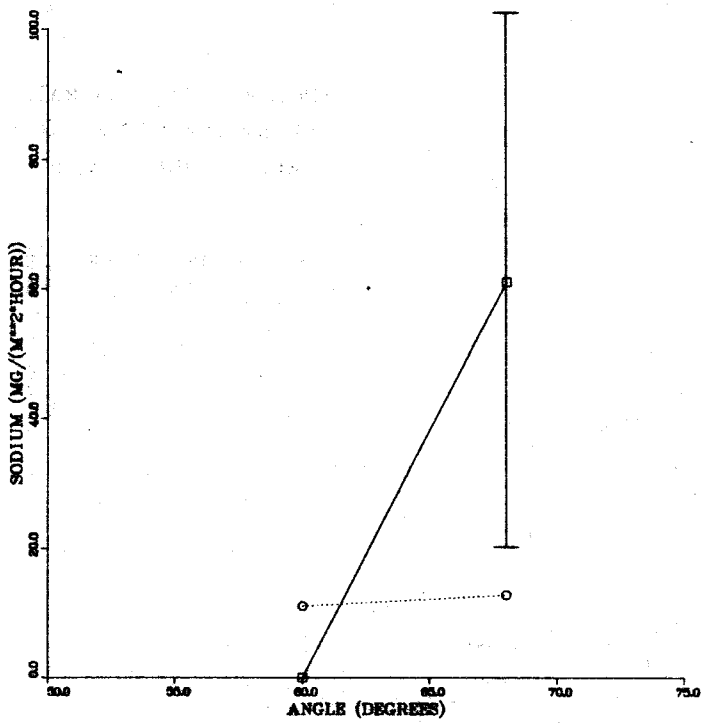

Figure 3-20. Comparison of ANL predicted and observed sodium deposition rate for Pittsburg California drift study of June 22, 1978.

Section 4

GENERAL CONCLUSIONS AND COMMENTS

From the above discussion, we can say that in four of the five data surveys used to test the ANL multiple-tower drift model, the model predicts sodium deposition rate within a factor of 3 at 50% of all ground samplers. Considering the weaknesses in the data pointed out earlier, this kind of performance provides good support for the model and quality of data as well. The good model/data comparisons do not provide definitive validation for the model, however. Field data acquired under widely differing environmental conditions and at different sites of multiple towers (natural as well as mechanical-draft towers) would provide a good complement to the Pittsburg data for model validation. Unfortunately, such data does not exist and is very expensive to acquire. As a consequence, we must rely more heavil on the accuracy of the theoretical assumptions made in the model. Certainly, no field data have been acquired beyond 1 km downwind of the Pittsburg towers; at and beyond those distances, we must rely exclusively on the accuracy of our theoretical assumptions for the physics of droplet dispersion, for those droplets that deposit beyond the 1 km distance.

Ongoing work is aimed at determining those conditions under which further simplifying assumptions in the theory may be justified. Such simplifications in the theory should also reflect savings in computer time. The first area relates to the droplet evaporation submodel. Three parameters have been defined which allow one to determine if the drop (a) goes only through Phase 1 (large drops), (b) spends a very small time in Phases 1 and 2, spending most of the time in Phase 3 (small drops), or (c) spends significant time in all three phases. Cases (a) and (b) can involve significant simplifications in droplet evaporation calculations and perhaps include 95% of all droplet sizes of interest. The three parameters mentioned above depend mainly on drop size, ambient relative humidity, and drop salt concentration. Any simplifications in determining distance to deposition for various drop sizes in different ambient environments will shorten computer run times of both our single and multiple-source drift codes. The second area of ongoing work relates to a study of the simplifications that may be possible in application of our multiple-source plume model. We are examining situations under which a simplified form of our multiple-source plume model may

still be accurate in predicting drift deposition; e.g., perhaps for two closely located natural-draft cooling towers. Such simplifications, if proved successful will make the computer model more efficient in its application to prototype problems.

The areas of ongoing work described above are specific to improving the single case models described in Volumes 1-5. However, there is a more important aspect to our future work and it relates to our imbedding these codes into our systematic methodology (1, 2) in which seasonal/annual plume and drift estimates can be made. That methodology is presently implemented as a package of 11 computer codes, several of which perform simple manipulations on available weather data and tower exit information. The analysis of cooling tower plume/drift impacts for a site can be carried out in a matter of several days with most of this time being spent in accumulating and organizing the various types of data. The cumulative computer time for all operations, except for plume and drift simulation, is less than 3 minutes per site on a CDC CYBER-175 (or IBM/3330) computer system. We estimate that the cost of executing the ANL plume and drift models (as described in these five volumes) as submodels to this methodology for a single site analysis with one set of cooling towers should be about 20 minutes on the CYBER-175 (or IBM/3330) The aim of this portion of our ongoing work then is (a) to refine and improve out existing seasonal/annual methodology as presented in References 1 and 2 and (b) to formally imbed the ANL plume/drift models into that system. That imbedding mostly involves a simple revision of input/output formats.

Since this Volume 5 is the last of the series, it is worth summarizing one final time the basic assumptions in our ANL models. Appendix A provides an outline of the theory of the models for such review purposes.

REFERENCES

1. W.E. Dunn. Predicting the Seasonal and Annual Impacts of Cooling Tower Plumes and Drift. Department of Mechanical and Industrial Engineering, University of Illinois at Urbana-Champaign. IAHR Cooling Tower Workshop. Sponsored by the Electric Power Research Institute. San Francisco, California. September 1980.

2. W.E. Dunn, A.J. Policastro, J. Ziebarth, S. Ziemer, and K. Haake. Appendix: Mathematical Modeling of Plumes from Proposed Cooling Towers at Seabrook and Alternative Sites. IN: Seabrook Alternative Site Study. NRC Staff Testimony

related to Alternative Sites to Seabrook Units 1 and 2. U.S. Nuclear Regulatory Commission. Office of Nuclear Reactor Regulation. December 1978.

Appendix A

REVIEW OF BASIC ASSUMPTIONS IN ANL PLUME/DRIFT MODELS

Although all parts of the ANL plume/drift model are described in various places in the five volumes, it is the purpose here to provide an outline of the complete (final) model. This outline is presented in terms of a listing of the key assumptions employed. Further details can be obtained by referring to the appropriate volume.

PLUME RISE MODELING

The basic assumptions are

- bent-over plume
- top-hat profiles of plume variables with determination of peak conditions by means of Gaussian profiles
- different spreading rates for momentum, temperature, and moisture
- empirical treatment of tower downwash through addition of a vertical downward pressure force to the plume and the addition of new entrainment when plume/tower wake interaction occurs. The additional dilution occurring during downwash was modeled by employing the empirical relations of Halitsky as a basis.
- plume merging methodology based on the theory of Wu and Koh. In this theory, the effects of wind direction on plume merging are accounted for.

Empirical coefficients used are

1. $\nu = 1.20$, the ratio of the momentum plume cross-sectional area to that of the temperature plume.
2. $\lambda = 0.51$, the ratio of the plume cross-sectional area of moisture to temperature plume.
3. $\alpha = 0.125$, $\beta = 0.575$. These are entrainment coefficients employed in our use of the Chan-Kennedy entrainment function.
4. $C_B = 0.34$, the constant in the treatment of the atmospheric diffusion phase.
5. $C_{wf} = 0.10$, $C_{wv} = 0.80$, and $C_L = 1.0$. C_{wf} is the coefficient for the downwash pressure force, C_{wv} is the downwash entrainment constant, and

C_L is the constant estimating the length of the tower wake cavity. C_{WV} is taken to be 0.40 for multiple-tower plumes (when one tower is in the wake of another).

DRIFT MODELING

The basic assumptions in modeling drift deposition are:

- droplets break away from the plume when they have fallen from the plume centerline a distance equal to the plume radius. [An alternative criterion developed by us provides a continuous transition between plume and ambient environment for the drift drops. Both criteria led to similar performance with Chalk Point data. The radius criterion, which is simpler to apply is presently employed in both single and multiple tower drift codes.]
- new droplet evaporation formulation which accounts for salt-concentration gradients within the drop.
- Ballistic methodology in treatment of droplet deposition (ignoring, at present, atmospheric turbulence effects).
- generalization of the sector-average concept in depositing drift when multiple sources are involved.
- droplets from every source are followed through to deposition; however, approximations for deposition distances are used based upon deposition information computed from the drift from the first source calculated.

No empirical constants are used to "tune" the drift model.

Note: The multiple-tower drift model contains the multiple-source plume model, the single-source plume model, and the single-source drift model as special cases. The multiple-source plume model contains the single-source plume model as a special case. The multiple-source drift model contains the single-source drift model as a special case.